2-P

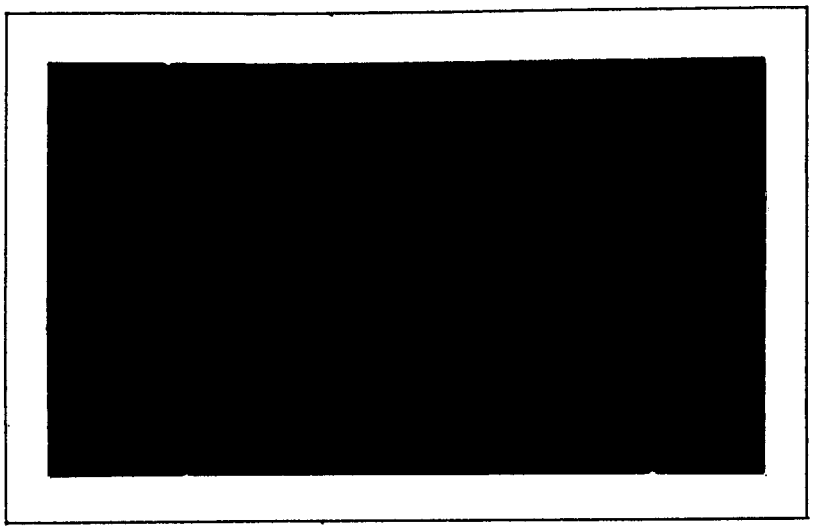

METALS RESEARCH LABORATORY

CARNEGIE INSTITUTE OF TECHNOLOGY

Carnegie-Mellon University

PITTSBURGH, PENNSYLVANIA

National Aeronautics and Space Administration
Research Grant NGR 39-087-003

Investigation of the Plastic Fracture of High Strength Steels

by

T. B. Cox and J. R. Low, Jr.

TR #4

Department of Metallurgy and Materials Science
Carnegie-Mellon University
Pittsburgh, Pennsylvania 15213

NASA Technical Report No. 4

October 1972

This investigation was made possible by a Research Grant from the National Aeronautics and Space Administration

INTRODUCTION

During the past few years, increased use has been made of high strength steels for critical structural applications in aircraft, naval vessels and aerospace vehicles. Unlike the low strength ferritic steels in which unstable fracture at low temperatures occurs by a cleavage process, these high strength alloys may fracture catastrophically by highly localized severe plastic deformation. The low strength ferritic steels generally exhibit a ductile to brittle transition over some temperature range below which brittle fracture occurs by cleavage and above which ductile fracture occurs by dimpled rupture[1] (plastic fracture). In most instances, the high strength alloy steels do not exhibit distinct ductile to brittle transitions and generally fail by dimpled rupture. Under loading conditions which impose high constraints on the high strength alloy, such as in thick sections or at the tips of crack-like flaws, fracture may occur at drastically reduced levels of macroscopic plastic strain with very little energy absorption, i.e., brittle fracture occurs.[2] While cleavage fracture has been extensively studied and many of the microstructural features which affect it have been determined, very little research has been done on the plastic fracture process in high strength steels. It is the purpose of this investigation to study in detail the three generally recognized stages of plastic fracture in high strength steels, namely, void initiation, void growth, and void coalescence. Armed with an understanding of the fracture process, it should be possible to suggest ways of improving the resistance of the high strength steels to plastic fracture.

The particular high strength steels being investigated in this study include plates from both commercial purity and high purity heats of AISI 4340 and 18 Ni, 200 grade maraging steels. All four alloys have been heat treated to yield strength levels of approximately 200 ksi. The values of fracture toughness of the steels fall in the order of:

Material	K_{Ic} (ksi$\sqrt{in}$)
Commercial AISI 4340	67.9
High Purity AISI 4340	97.2
Commercial 18 Ni Maraging	110.0
High Purity 18 Ni Maraging	149.1*

* This value was determined from invalid tests due to undersized specimens

Results of the progress of this investigation prior to the current report period are presented in detail elsewhere,[3] but will be reviewed briefly here.

A quantitative metallographic investigation has been completed and the inclusion populations in the four steels have been described. For both alloy systems, the number of non-metallic inclusions per unit volume of steel is larger in the high purity plates, but the volume fraction of inclusions and the average size of the inclusions are larger in the commercial grade plates. Using a scanning electron microscope equipped with an X-ray energy dispersive analyzer together with observations made using light microscopy, it was determined that the predominate inclusion type in the AISI 4340 alloys is manganese sulfide, generally present in the geometric shape of ellipsoids whose three axes are unequal. The sulfides apparently are nucleated in the melt on particles which are products of the deoxidation process, since they have been shown to contain

calcium and aluminum. The predominate inclusion type in the 200 grade maraging steels is a cuboidal titanium carbo-nitride.

A fractographic study was carried out using fracture surfaces produced in both fracture toughness and tensile tests. Electron fractographs of replicas taken from the regions of fast fracture initiation on compact tension fracture toughness specimens and the central regions of normal rupture on round tensile specimens revealed that the fracture surface features in these areas were identical for both tests. The fracture surfaces of the maraging steels were composed entirely of large dimples, while the fracture surfaces of the AISI 4340 steels exhibited only small area fractions of large dimples with over 90 percent of the fracture surface areas composed of very small dimples, one-to-two orders of magnitude smaller than the large dimples. It was established that the center-to-center distances of large dimples on the fracture surfaces of all the alloys roughly corresponded with the values of inclusion spacings determined by quantitative metallography. This fact, together with the observed frequent association of fractured inclusions and large dimples on the fracture surfaces, leads to the conclusion that the large voids are nucleated by the non-metallic inclusions in these alloys. By the use of extraction replicas taken off tensile fracture surfaces and selected area electron diffraction, it was established that the small dimples found on the fracture surfaces of the AISI 4340 alloys are associated with the small, strengthening carbides in the quenched and tempered structure which act as nucleating particles for void formation.

Work completed subsequent to the results outlined above and reported herein consists of a metallographic investigation of strained and sectioned tensile specimens with the object of:

1. Qualitatively describing the fracture process in smooth tensile specimens of these alloys.
2. Quantitatively describing the void nucleation and growth stages of fracture.
3. Determining which aspects of the fracture processes in these alloys result in observed differences in fracture toughness.

TENSILE FLOW PROPERTIES

As previously reported,[3] it was observed that for any one of the four alloys the fracture surface features in the region of fast fracture initiation in K_{Ic} specimens were the same as those from the central region of normal rupture in smooth, round tensile specimens. These observations suggest that the initial or critical processes which lead to fracture are similar for the two specimen geometries in these particular alloys. While precracked fracture toughness specimens are meant to simulate flawed material in service, they are expensive to produce; and it is generally quite difficult to arrest the fracture process once it has begun. Thus, it was decided to study the initiation and progression of plastic fracture in smooth, round tensile specimens with the belief, based on the previous fractographic observations, that the observed process would be comparable to that taking place at the tip of a crack.

The general procedure for this part of the investigation was to load a tensile specimen to some predetermined level of plastic strain, unload and section the specimen longitudinally, exposing the longitudinal midplane to metallographic examination. One tensile specimen of each alloy was strained to fracture in order to determine the tensile flow properties of the alloys and to provide initially several metallographic specimens (the broken tensile halves) of each alloy for determining the most advantageous orientation of the midplane for observing voids (either perpendicular or parallel to the primary rolling direction). The tension specimens were standard smooth, round specimens 1/4 inch in diameter. Both the specimen geometry and the testing procedure were in accordance

with ASTM standard E8-61T on tension testing of metallic materials. For the tension tests, the strain was monitored by periodically measuring the specimen diameter using a point micrometer. The tensile specimens were taken from the four plates in the transverse direction (tensile axis transverse to the primary rolling direction, but lying in the plane of the plate) to correspond with the orientation of the previous fracture toughness specimens. The stress-strain curves for the four alloys are presented in Figures 1-4 together with the uniaxial flow curves determined using the Bridgman correction for necking.(4)

It was found that in the plastic range, the flow curves of the four alloys could be fit reasonably well to the exponential form:

$$\sigma = k\epsilon^n$$

The values of the strain hardening exponent n together with the other pertinent tensile properties of the alloys determined in these single tests are summarized in Table I. There are several observations to be made regarding the macroscopic plastic flow characteristics of these alloys which undoubtedly influence the fracture process. Although the strength levels for the two alloy systems are slightly different, the strains at which necking begins as determined at the maximum load are about the same for all four alloys; that is, a strain of approximately two percent. However, the values of true strain-to-fracture vary widely and correspond to the established order of fracture toughness levels; namely, continuously increasing from the least tough alloy (commercial grade AISI 4340) to the high purity AISI 4340 to the commercial grade 18 Ni maraging and ending with the toughest alloy (high purity 18 Ni

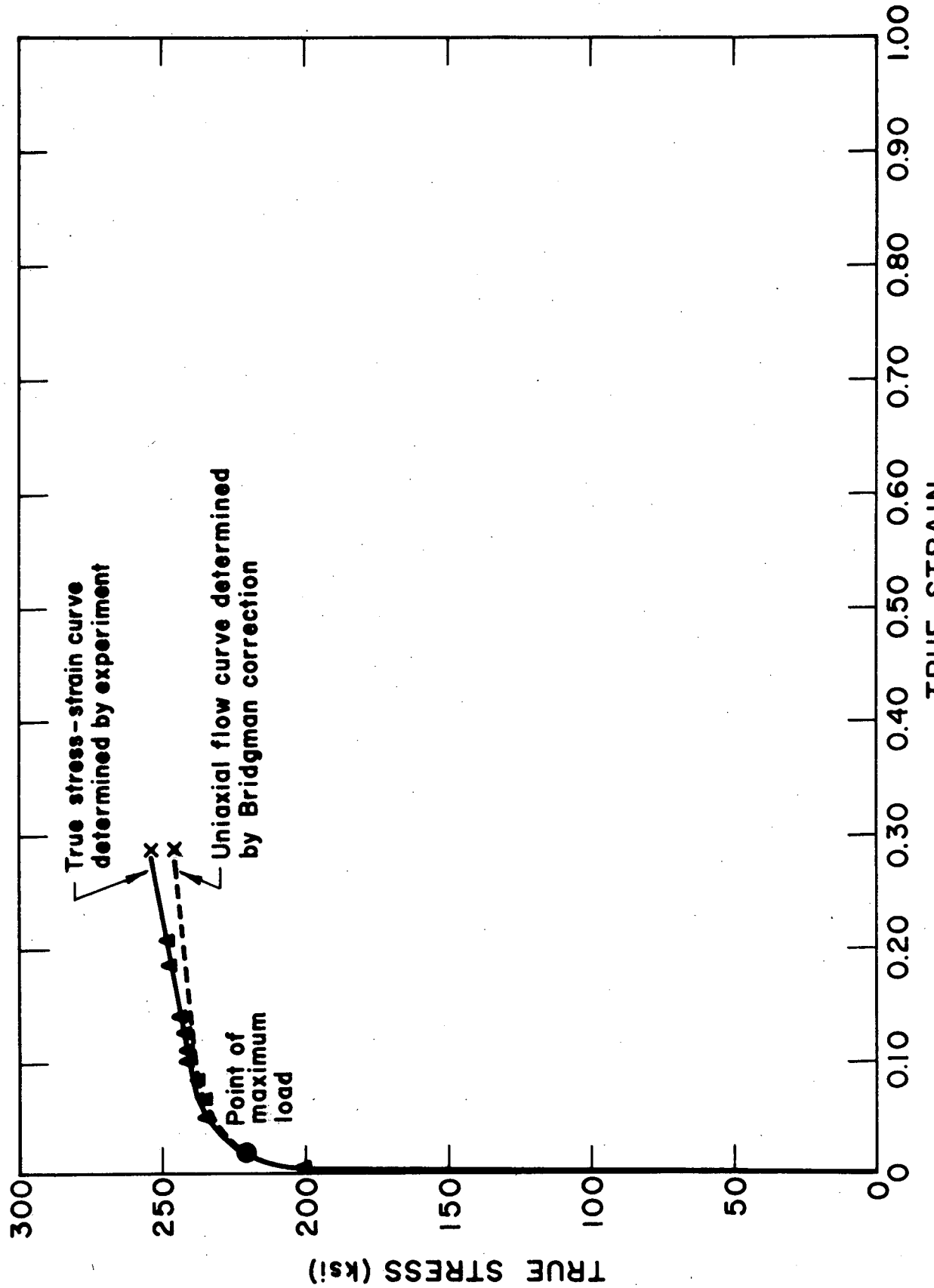

Figure 1 Tensile Curve for Commercial AISI 4340

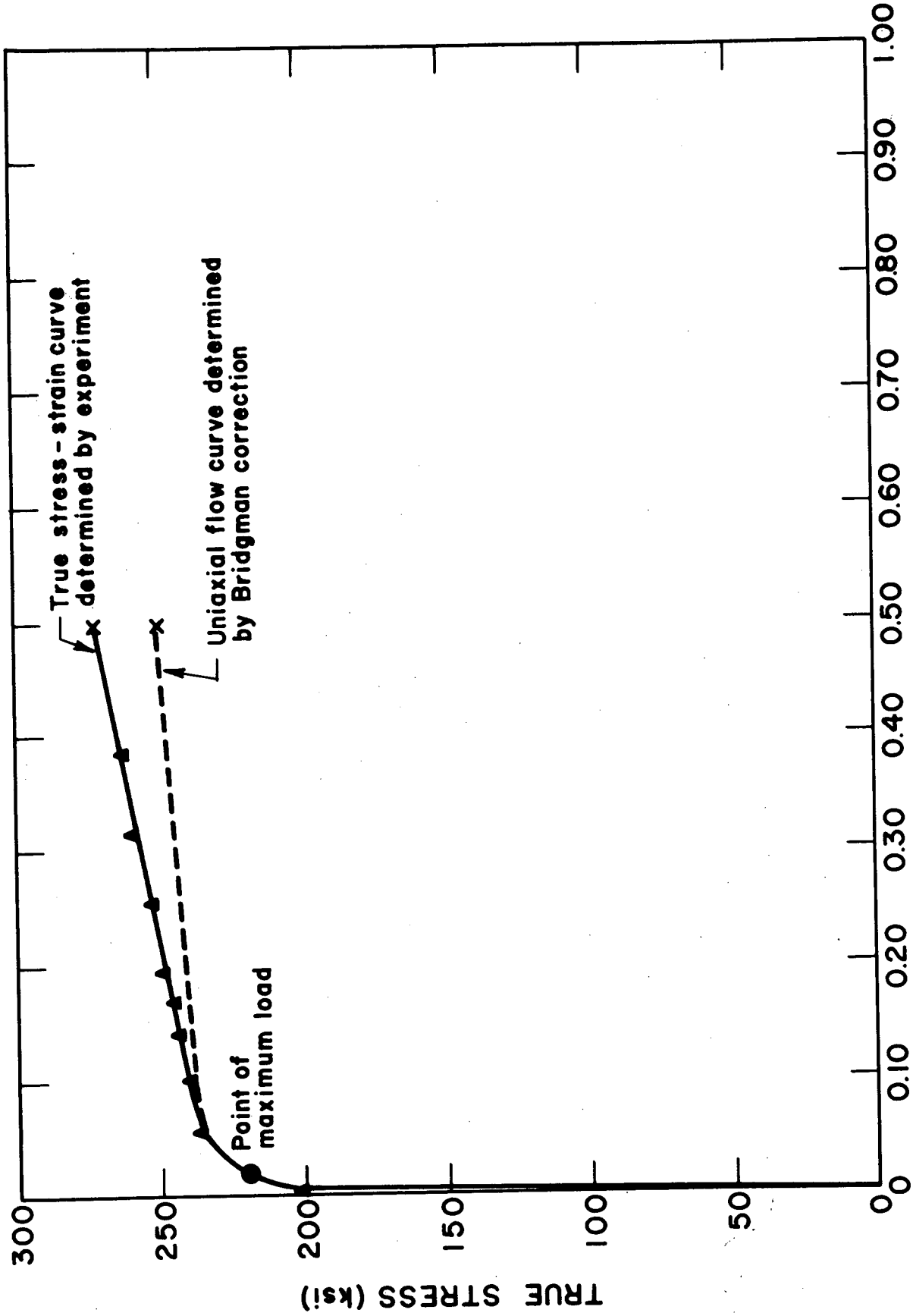

Figure 2 Tensile Curve for High Purity AISI 4340

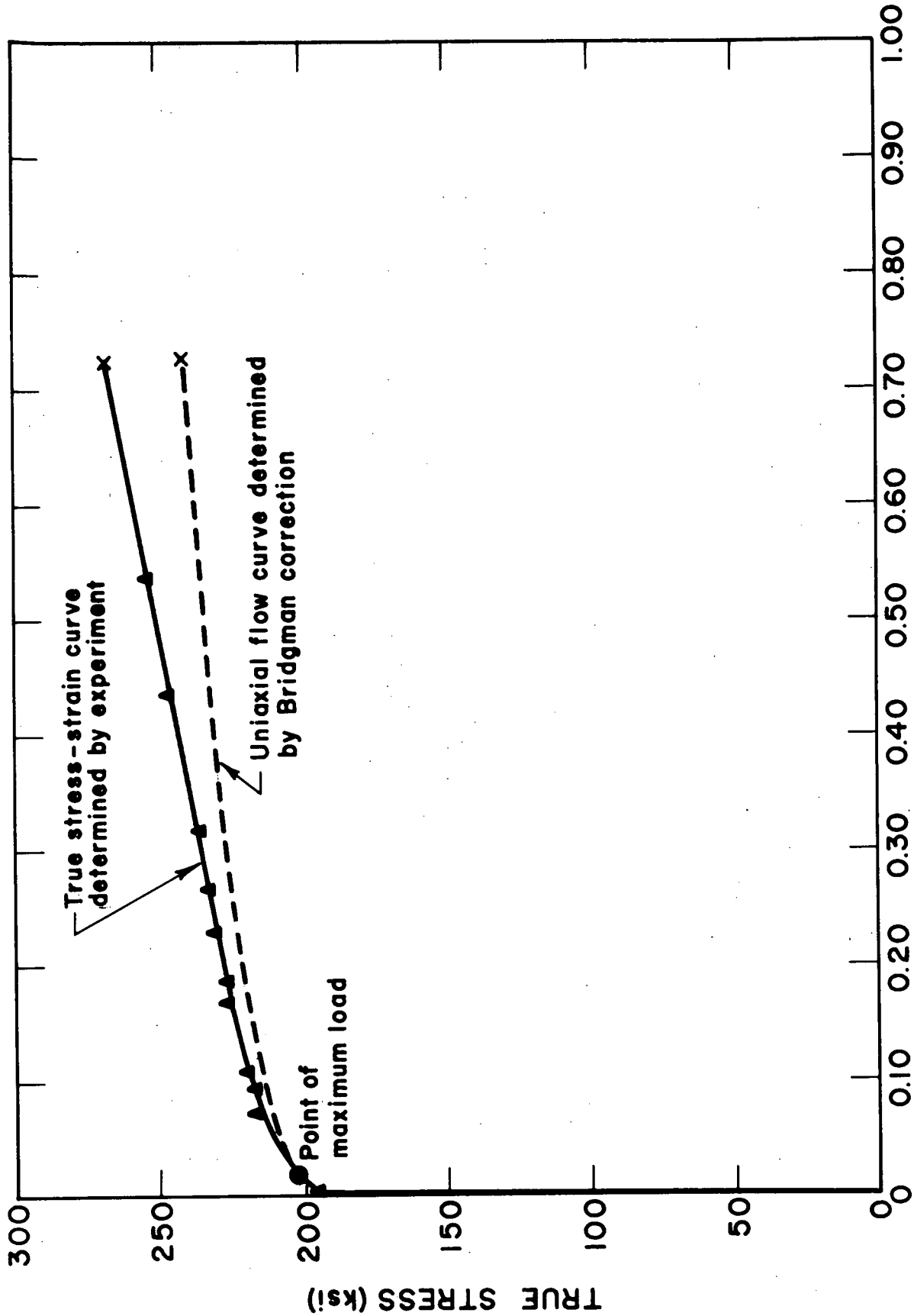

Figure 3 Tensile Curve for Commercial 18 Ni Maraging

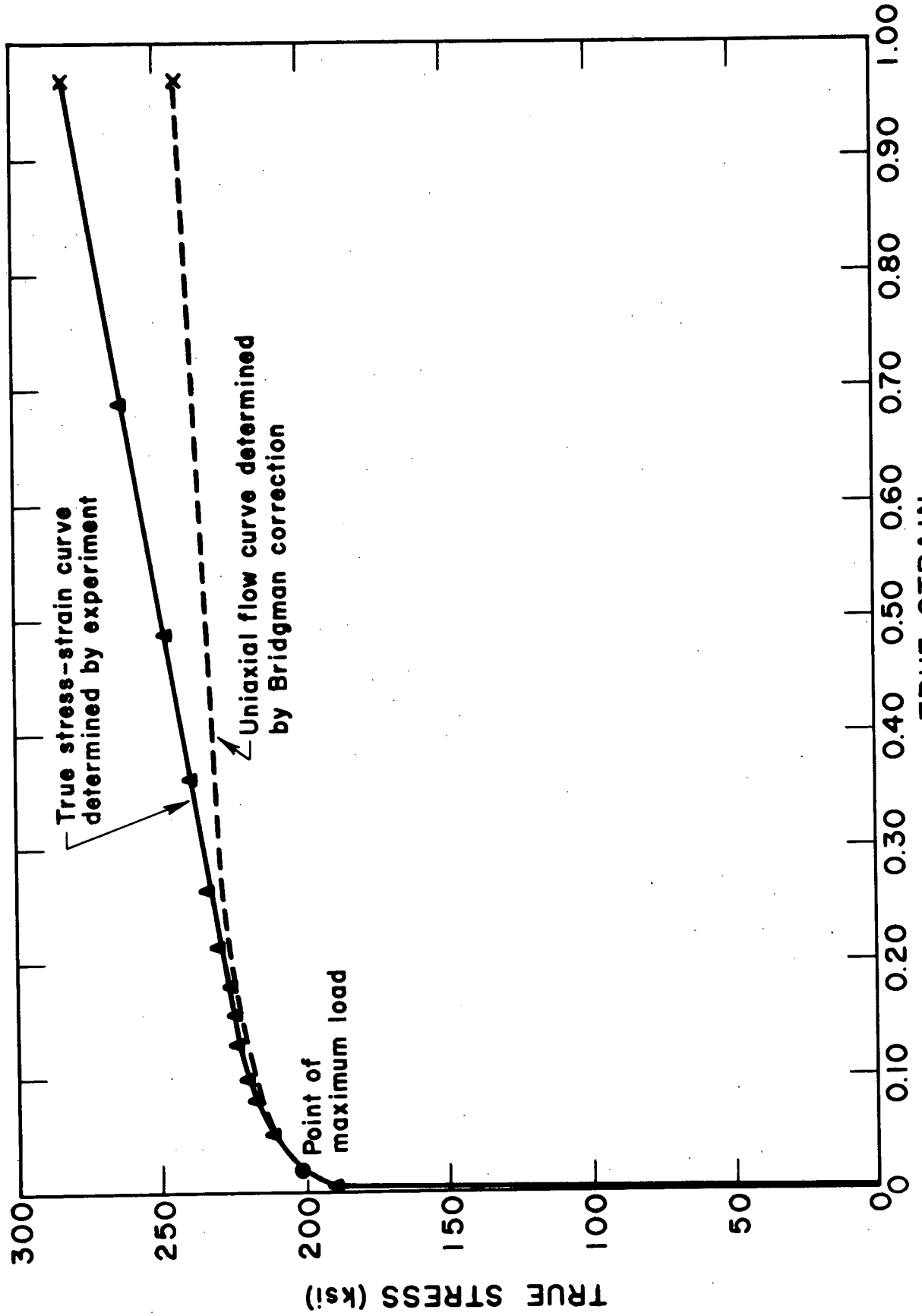

Figure 4 Tensile Curve for High Purity 18 Ni Maraging

TABLE I

Room Temperature Tensile Properties of High Strength Steels

	Commercial AISI 4340	High Purity AISI 4340	Commercial 18 Ni	High Purity 18 Ni
Yield Strength 0.2% Offset (ksi)	204.8	203.8	193.7	188.5
Ultimate Tensile Strength (ksi)	221.8	219.2	198.0	198.7
True Strain at Necking	0.019	0.017	0.018	0.017
True Strain to Fracture	0.288	0.498	0.728	0.970
Strain Hardening Exponent	0.032	0.029	0.062	0.055

maraging steel). The plastic flow characteristics as described by the strain hardening exponent are not affected by the level of purity but are different for the two alloy systems. The maraging steels exhibit higher values of n than do the quenched and tempered AISI 4340 alloys, indicating a greater ability to work harden. It should be noted that the values of n were determined using stresses which were corrected for necking and only data which were taken at strains beyond necking. This procedure may account for the fact that the values of n do not correspond to the values of the true strain at necking as predicted by Considère.[20] The forms of the stress-strain curves are the same for all four alloys, exhibiting a shallow, almost linear slope in the plastic range from just beyond necking to failure. The maraging steels show an ability to withstand more plastic strain before fracture than do the AISI 4340 alloys, even more than would be expected due to the slight difference in yield strength. Apparently, the flow characteristics of the two alloy systems are not too much different, at least from a macroscopic standpoint. The main difference in their deformation behavior lies in the premature interruption of the plastic deformation of AISI 4340 by the fracture process.

METALLOGRAPHIC SPECIMEN PREPARATION

As for the determination of the flow curves of the four alloys, standard smooth, round tensile specimens 1/4 inch in diameter were also used for the metallographic investigation. The tensile axis was taken transverse to the primary rolling direction with the specimens lying in the plane of the plate. Specimens were strained to various levels of plastic strain, chosen to cover the entire plastic strain history of each alloy from necking to failure. The lower limit to the plastic strains was chosen as the necking strain, since it was observed that no appreciable void initiation occurred at stresses below the ultimate tensile stress.

The necked specimens were then prepared for metallography. Based on the observations made on sections of the fractured tensile halves, it was decided to surface grind the necked sections to within 0.075 mm (3 mils) of the mid-point of the minimum diameter of the neck. Experience indicated that using automated polishing equipment the final metallographic polishing would remove approximately 0.075 mm (3 mils) and thus the above procedure would permit viewing of the longitudinal midplane of each specimen. The grinding was done such that the plane exposed was perpendicular to the primary rolling direction and parallel to the tensile axis. This particular orientation was found to offer the most advantageous view of voids in the AISI 4340 alloys due to the elongation of the sulfides perpendicular to the section plane. Orientation made no difference with the 18 Ni maraging steels, since the carbo-nitride particles had no preferred orientation. The orientation of the tensile specimens during testing and the orientation of the sectioning process are illustrated in Figure 5.

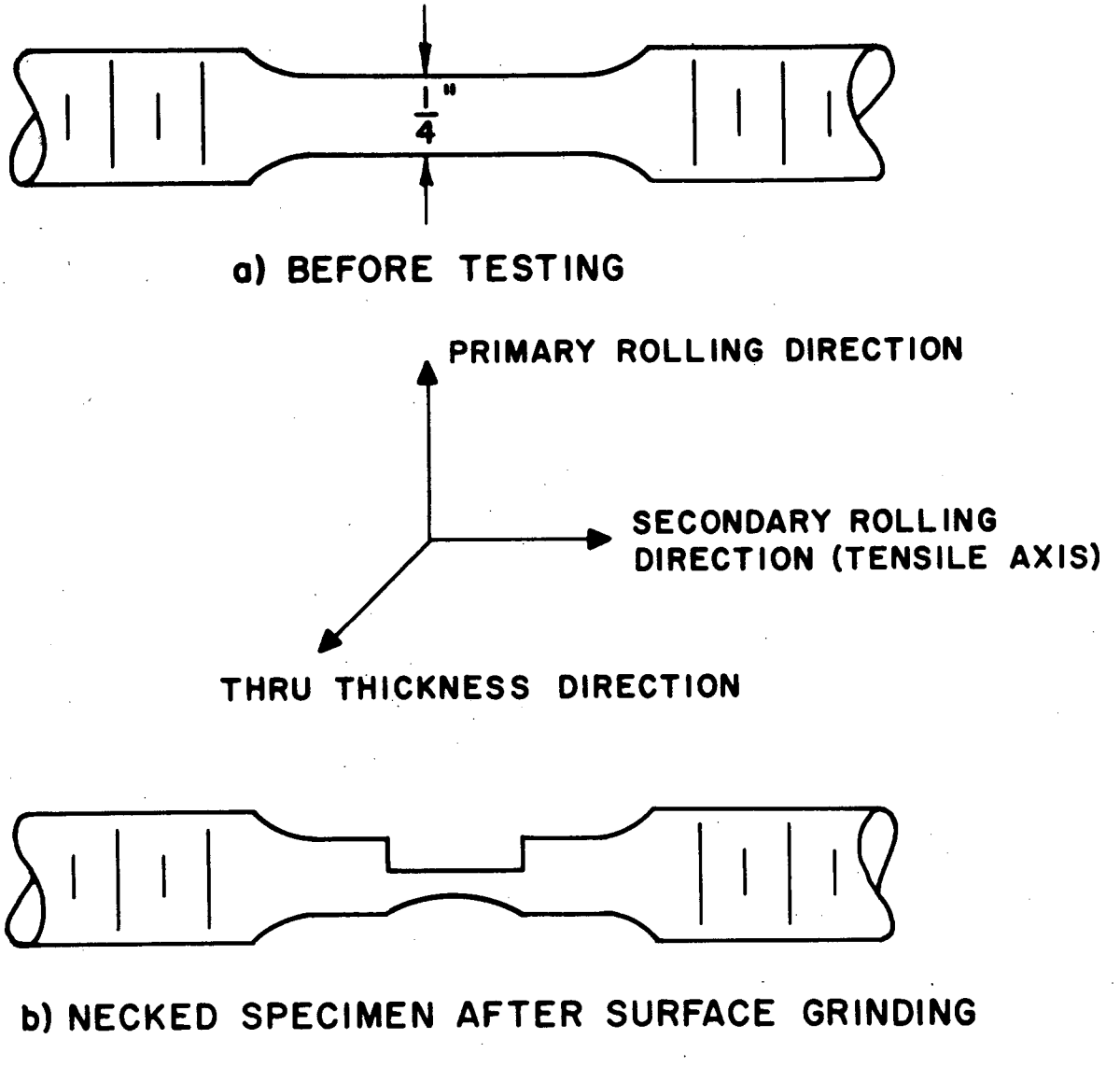

Figure 5 Orientation of Tensile Specimens and Section Plane

Once a specimen was surface ground as illustrated, the neck was cut from the tensile specimen using an abrasive cut-off wheel and mounted so as to expose the ground plane. Final polishing was carried out using automated equipment and 240, 320, 400, and 600 grit silicon carbide abrasive papers; 6, 3, and 1 micron diamond paste; and finally 0.05 micron alumina powder. This procedure, as stated above, removed 0.075 mm (3 mils) of the specimen thus exposing the longitudinal midplane of the neck. This technique resulted in no noticeable distortion of voids or any pulling out of inclusions from the matrix. The specimens were then studied extensively in the unetched condition using light microscopy.

VOID INITIATION

As demonstrated previously [3] and as illustrated in Figure 6, the fracture surfaces of the AISI 4340 alloys were covered by two populations of dimples. A series of large dimples as at "A" in Figure 6 which are nucleated by sulfide inclusions are separated by regions of fine dimples as at "B" in Figure 6 which were shown to be nucleated by carbide particles. The results of the current investigation indicate that the large voids nucleated at the sulfides are initiated almost exclusively by separation of the sulfide-matrix interface. No appreciable void formation was detected at stresses lower than the ultimate tensile stress. Figure 7 presents examples of void initiation at sulfide inclusions, in both high purity (7a) and commercial grade (7b) AISI 4340 alloys. (The newly initiated voids are indicated by arrows.)

Only occasionally were sites other than the sulfide-matrix interface observed to nucleate the large voids in the AISI 4340 alloys. However, these other nucleation sites (described below) were also always associated with the sulfide particles. Occasionally with very large sulfides containing a large nucleating particle, voids were observed to form by fracturing of the sulfide along the boundary between the sulfide and the interior nucleating particle. An example of this type of nucleation is presented in Figure 8a. Very long, thin sulfides oriented along the tensile axis were sometimes found to be fractured across a minimum section as illustrated in Figure 8b. Neither of these nucleating mechanisms was seen often, but rather the predominate mechanism of sulfide-matrix interface failure provided most of the large void nucleation. It should also be

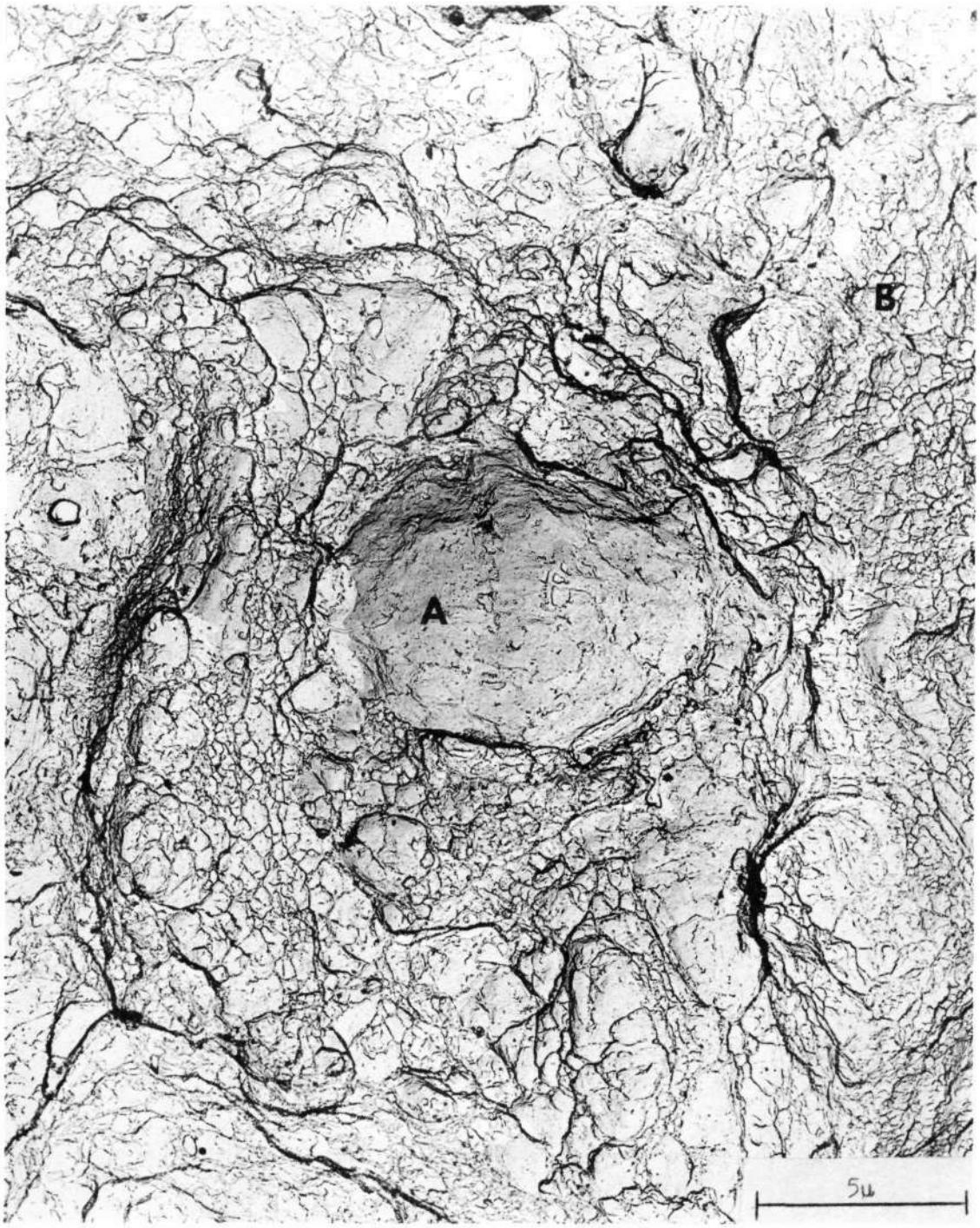

Figure 6 Fractograph Taken Adjacent to Fatigue Crack on K_{Ic} Specimen of Commercial Purity AISI 4340 ("A" indicates region of large dimple and "B" indicates region of small dimples.)

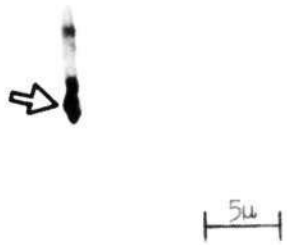

a. High Purity AISI 4340
Loaded Beyond Ultimate
Tensile Stress
(ϵ = 0.057)

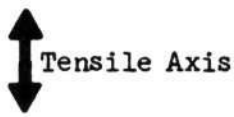

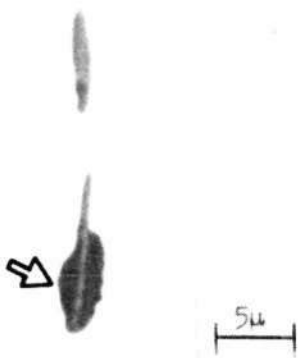

b. Commercial AISI 4340
Loaded to Ultimate
Tensile Stress
(ϵ = 0.018)

Figure 7 Examples of Void Initiation by Interface Separation at the Matrix-Sulfide Interface in AISI 4340 Plastically Strained (Arrows indicate voids)

a. Void Initiation by Rupture of Sulfide-Nucleating Particle Interface

Tensile Axis

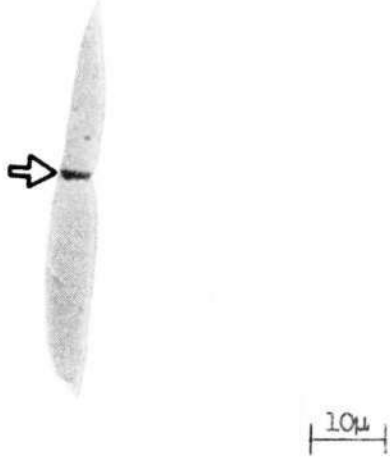

b. Void Initiation by Fracture of Sulfide

Figure 8 Examples of Abnormal Nucleation Sites for Large Voids in AISI 4340 Strained Plastically (Voids indicated by arrows)

pointed out that the largest inclusions nucleated voids first, i.e., at lower strains. As straining proceeded, smaller inclusions would then begin to nucleate voids so that the nucleation process continued throughout the entire strain history of the alloy with progressively smaller inclusions acting as nucleating sites for voids.

While it was previously established that the small dimples on fracture surfaces of the AISI 4340 steels are nucleated by carbide particles, it was not known exactly how the voids were nucleated, i.e., by interface separation between the carbide and the matrix or by fracture of the carbide. In order to establish the exact mechanism of void nucleation at the carbides, a series of thin foils were prepared from near the fracture surfaces of broken AISI 4340 tensile specimens. The foils were made by hand grinding on abrasive papers from opposite directions in order to produce sections of the longitudinal midplane approximately 0.075 mm (3 mils) thick. These mechanically produced foils were then electrolytically thinned in a 10% solution of perchloric acid in glacial acetic acid until they were thin enough for electron transmission.

Evidence was found that the small voids are nucleated by decohesion of the carbide-matrix interface. Figure 9 presents two observed examples of voids formed at carbide interfaces. The voids are indicated by the arrows and the carbides by the letter "C". Selected area electron diffraction confirmed these particles to be cementite.

As illustrated in Figure 10, the fracture surfaces of the 18 Ni maraging steels have been shown to be composed almost entirely of large dimples. These dimples have been shown to be nucleated by carbo-nitride

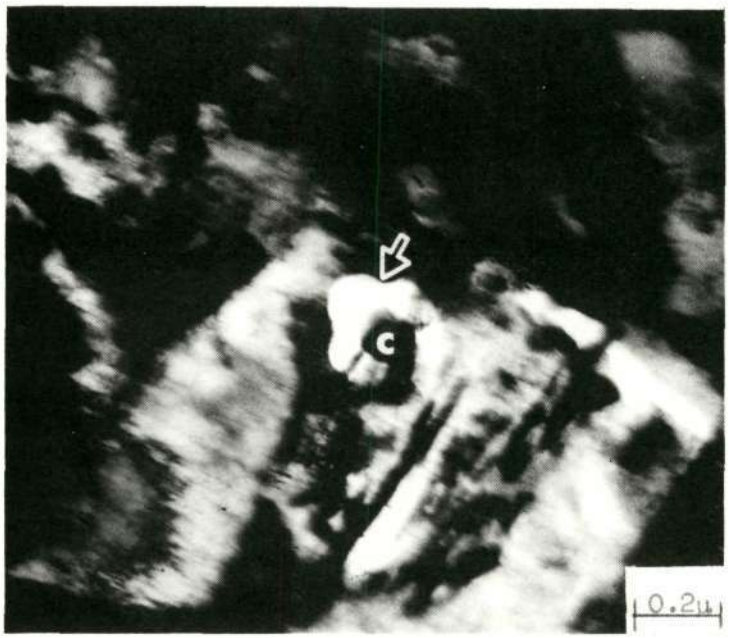

Figure 9 Void Initiation by Decohesion of Carbide-Matrix Interfaces in AISI 4340 Plastically Strained (Arrow indicates void and "C" indicates carbide)

Figure 10 Fractograph Taken Adjacent to Fatigue Crack on K_{Ic} Specimen of High Purity 18 Ni Maraging Steel ("X" indicates cleaved titanium carbo-nitride at bottom of large dimple)

inclusions. An example of a cleaved carbo-nitride inclusion lying in the bottom of a large dimple is indicated at "X" in Figure 10. The current metallographic investigation has demonstrated that the voids in these maraging alloys are nucleated exclusively by fracturing of the carbo-nitride inclusions. Examples of cracked carbo-nitride particles in both high purity (11a) and commercial grade (11b) maraging steels strained plastically are presented in Figure 11. As in the AISI 4340 steels, the larger carbo-nitride inclusions in the maraging steels cracked first, i.e., at lower strains. The process of cracking of inclusions continued as the strain increased with smaller and smaller inclusions continuing to fail.

The metallographic investigation of the void nucleation process in these alloys has revealed a fundamental difference in void nucleation processes between the AISI 4340 alloys and the 18 Ni, 200 grade maraging steels. Both populations of voids in the AISI 4340 alloys, i.e., both large and small voids, are initiated by decohesion at the interface between second phase particles and the matrix. On the other hand, the voids in the maraging steels are nucleated by cracking of titanium carbo-nitride inclusions. In both alloy systems, the nucleation of voids at non-metallic inclusions occurs only after the steels have been strained plastically to levels approximately those of the necking strains, i.e., loaded to the ultimate tensile stress. While no detailed study has been made during straining of the progression of small void initiation at the carbides in the AISI 4340 alloys due to the difficulty of the observations, it has been found that void initiation at non-metallic inclusions continues

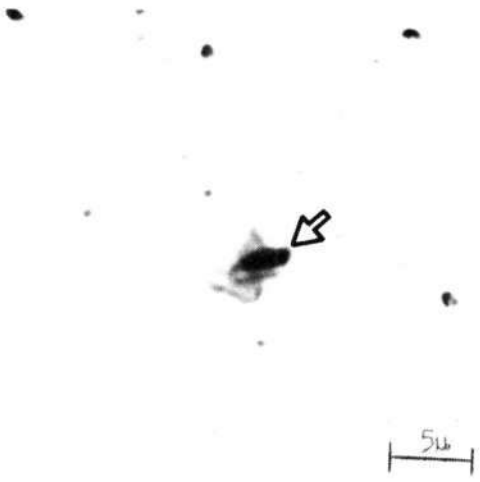

a. High Purity 18 Ni Maraging Loaded Beyond the Ultimate Tensile Stress (ϵ = 0.049)

Tensile Axis

b. Commercial 18 Ni Maraging Loaded to Ultimate Tensile Stress (ϵ = 0.018)

Figure 11 Examples of Void Initiation by Fracture of Carbo-Nitride Inclusions in 18 Ni, 200 Grade Maraging Steel Plastically Strained (arrows indicate voids)

throughout the strain history of each of the four steels. In all alloys, the largest inclusions initiate voids at lower strains regardless of whether the interface fails or the particle fractures. As straining proceeds, smaller and smaller inclusions begin acting as sites for void initiation.

VOID GROWTH

As the strains are increased beyond necking in these alloys, the voids which have been initiated at non-metallic inclusions grow by some mechanism involving plastic flow of the matrix. The series of photomicrographs in Figures 12-14 illustrate the progressive increase in both the number and size of voids in the necked region of commercial AISI 4340 specimens as the strain is increased. The increase in the number of voids as the strain increases is the result of continuing void initiation at smaller and smaller inclusions, as noted above; while the increasing size of the voids is the result of progressive void growth. These two simultaneously occurring processes result in a wide spread in the sizes of voids present.

Examination of Figures 12-14 further reveals that the larger voids appear to be found in the center of the specimen with the sizes of voids generally decreasing as one moves away from the center line. The general shapes of voids also change from edge to center of the midplane at high strains. In the centers of the specimens, the voids show a tendency to grow in both the direction of the tensile axis and in the radial direction (perpendicular to the tensile axis). Examples of voids in the central portion of tensile specimens of commercial grade AISI 4340 which have grown during straining are presented in Figure 15. It should be noted that at small strains (15a), the voids in the center show little sideways growth, rather they tend to grow preferentially in the direction of the applied tensile stress. However, as the strain increases (15b and 15c), the voids in the central region of the neck grow both longitudinally

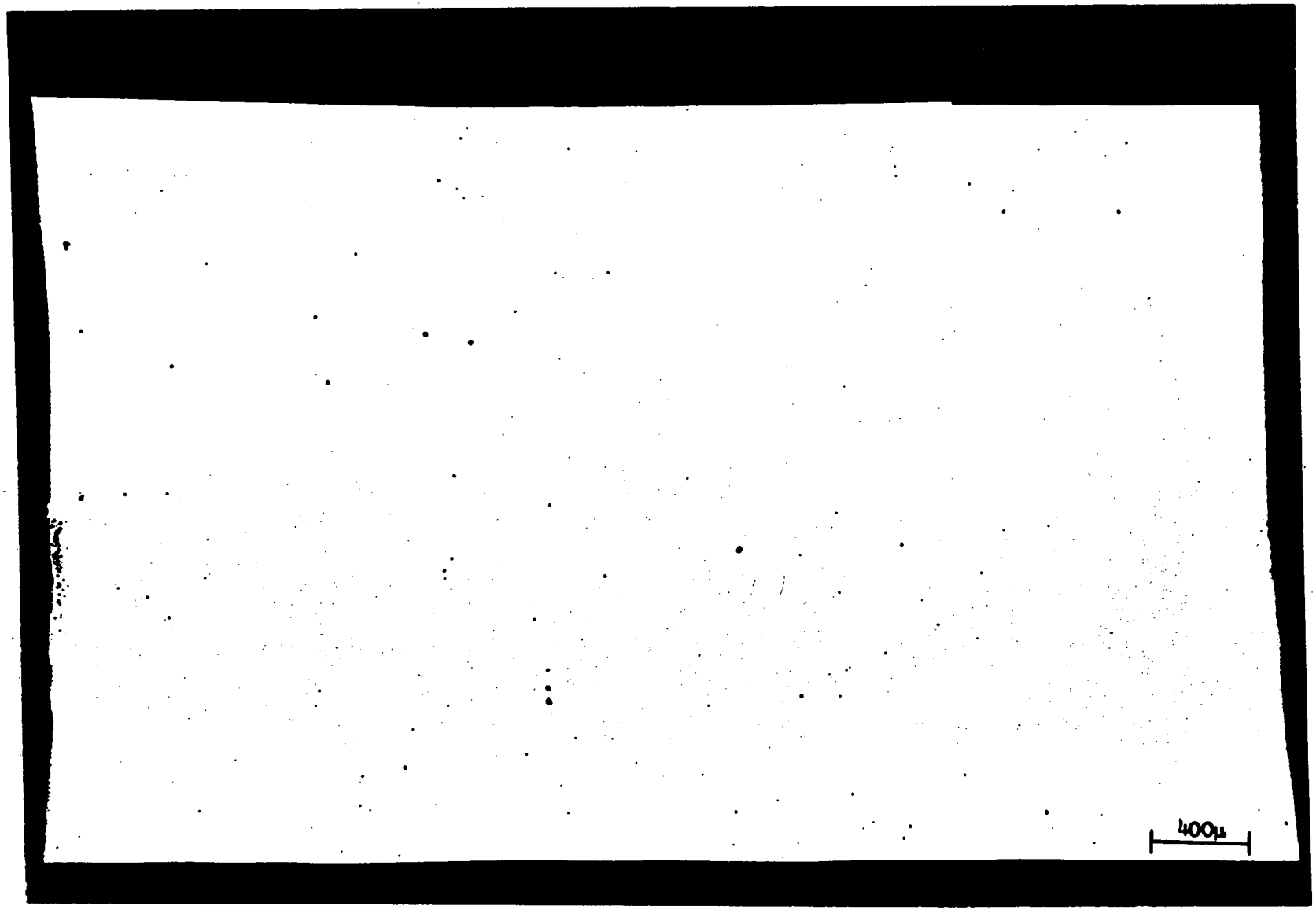

Figure 12 Midplane of Neck of Commercial AISI 4340
Plastically Strained 9 Percent

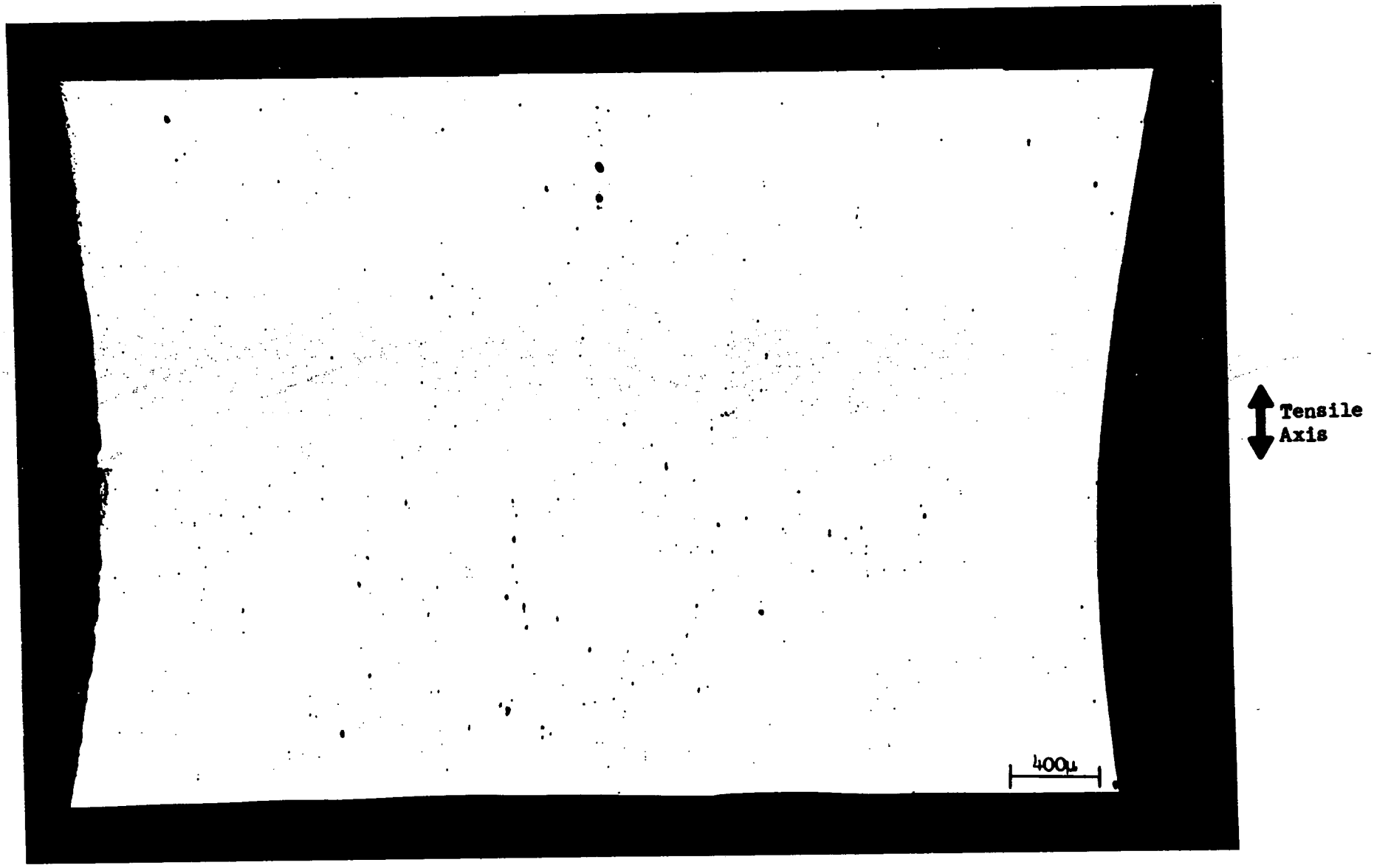

Figure 13 Midplane of Neck of Commercial AISI 4340
Plastically Strained 14 Percent

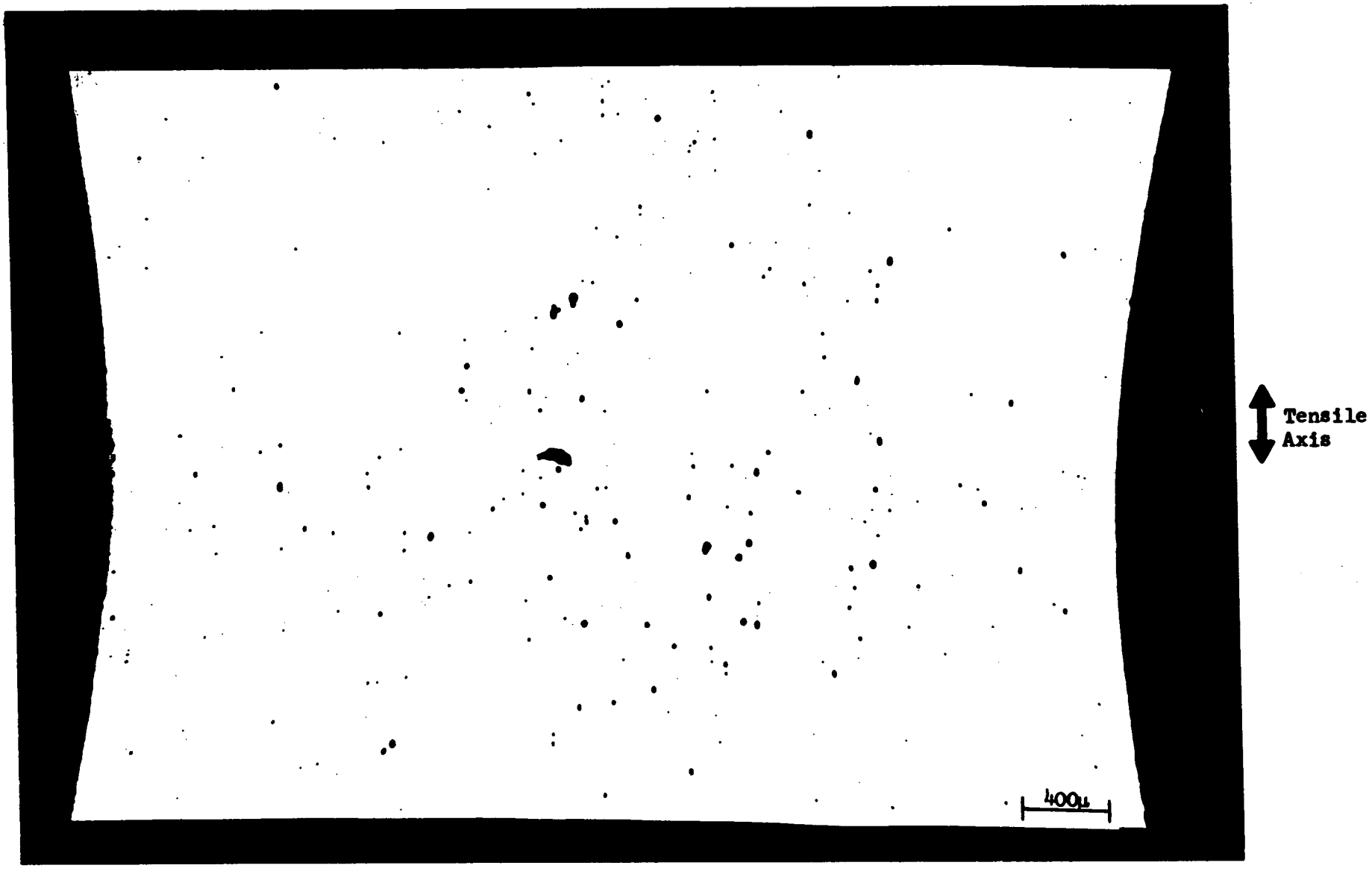

Figure 14 Midplane of Neck of Commercial AISI 4340
Plastically Strained 25 Percent

10μ

a. Plastically Strained
9 Percent

10μ

b. Plastically Strained
17 Percent

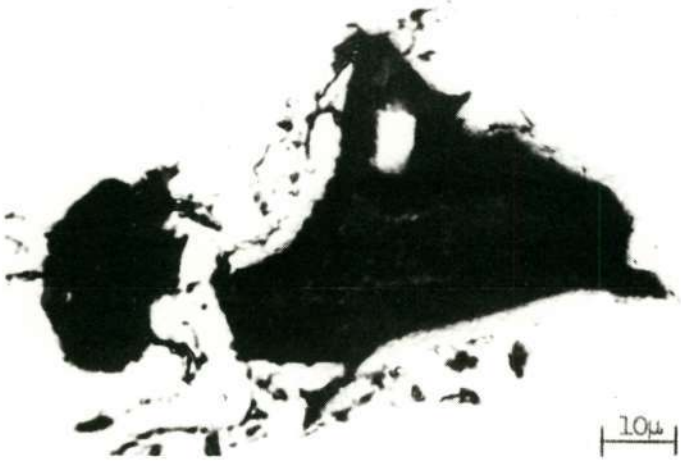

10μ

Tensile Axis

c. Plastically Strained
26 Percent

Figure 15 Voids in the Centers of Tensile Specimens of Commercial AISI 4340 Plastically Strained

and laterally. It has also been observed that voids which are nucleated outside the necked region, i.e., removed from the minimum specimen diameter in the longitudinal direction, tend to show little lateral growth even at high strains. Likewise, voids towards the edges of the specimens also tend to lack evidence of appreciable growth in the radial direction even at high strains. These voids tend to be elongated in the direction of the tensile axis and are generally no wider than the nucleating sulfide. Examples of elongated voids near the edges of tensile specimens of commercial grade AISI 4340 strained plastically are presented in Figure 16. Apparently, the larger degree of triaxial stress in the center of the neck which develops at high strains aids the lateral growth of the voids.

While all of the examples of the void growth process in AISI 4340 presented above have been for the commercial alloy, the same observations were also made in the high purity AISI 4340 alloy so that the void growth process is qualitatively the same for both alloys.

The general metallographic description of the growth process in both the maraging alloys is similar to that presented above for the quenched and tempered AISI 4340 alloys. Both maraging alloys behave similarly although the illustrations below will be made using the results for the commercial alloy only. The general increase in the size and number of voids on the midplane of the neck with increasing strain may be readily seen in Figures 17-19. From these photomicrographs, it is also possible to see that the voids in the central portions of the neck seem to be larger than those near the edge, especially at larger strains. Similar to the behavior found in the AISI 4340 alloys, voids in the

10μ

a. Strained Plastically
17 Percent

Tensile Axis

10μ

b. Strained Plastically
25 Percent

Figure 16 Voids on the Edges of Tensile Specimens of Commercial AISI 4340 Plastically Strained

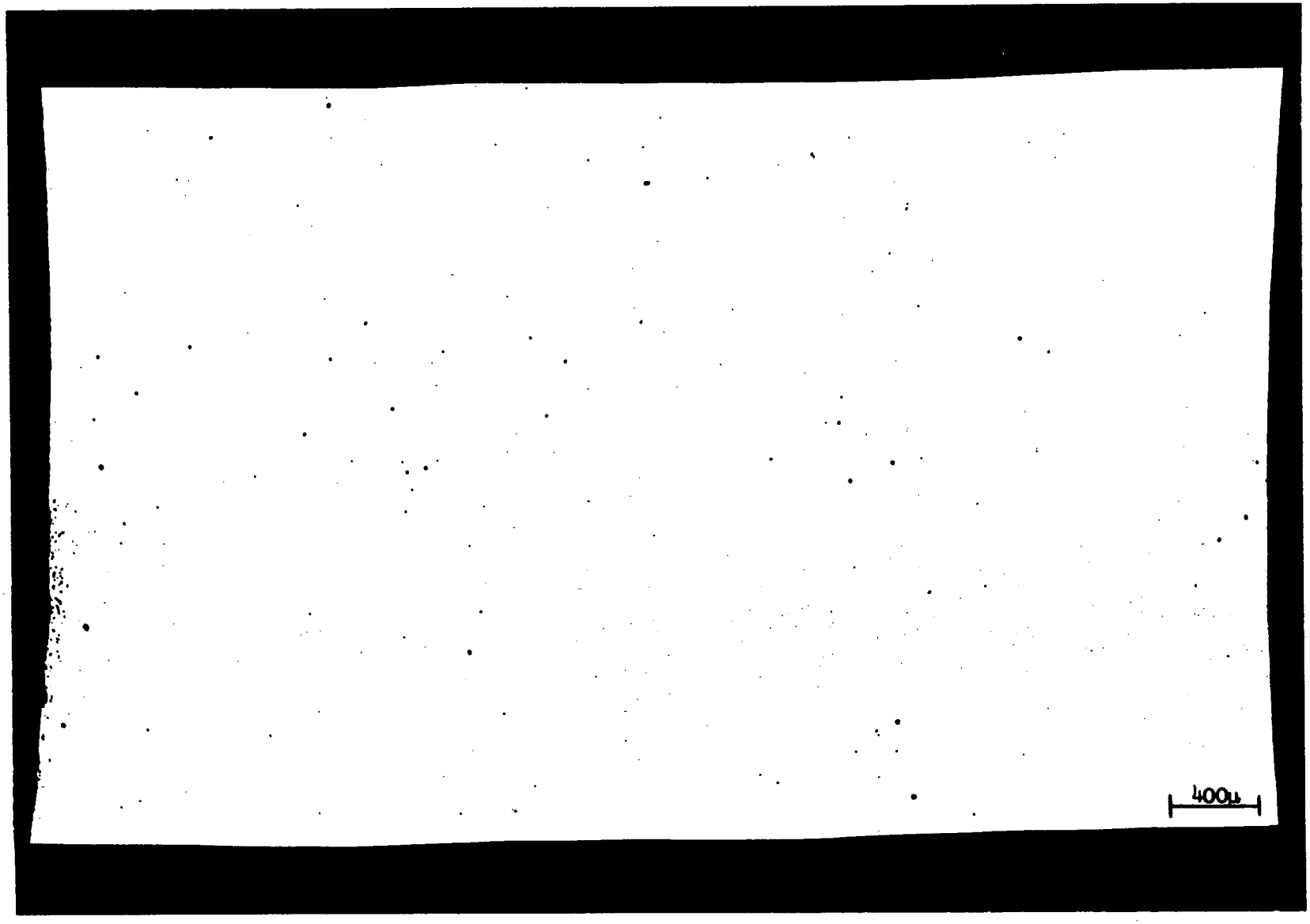

Figure 17 Midplane of Neck of Commercial 18 Ni Maraging Plastically Strained 18 Percent

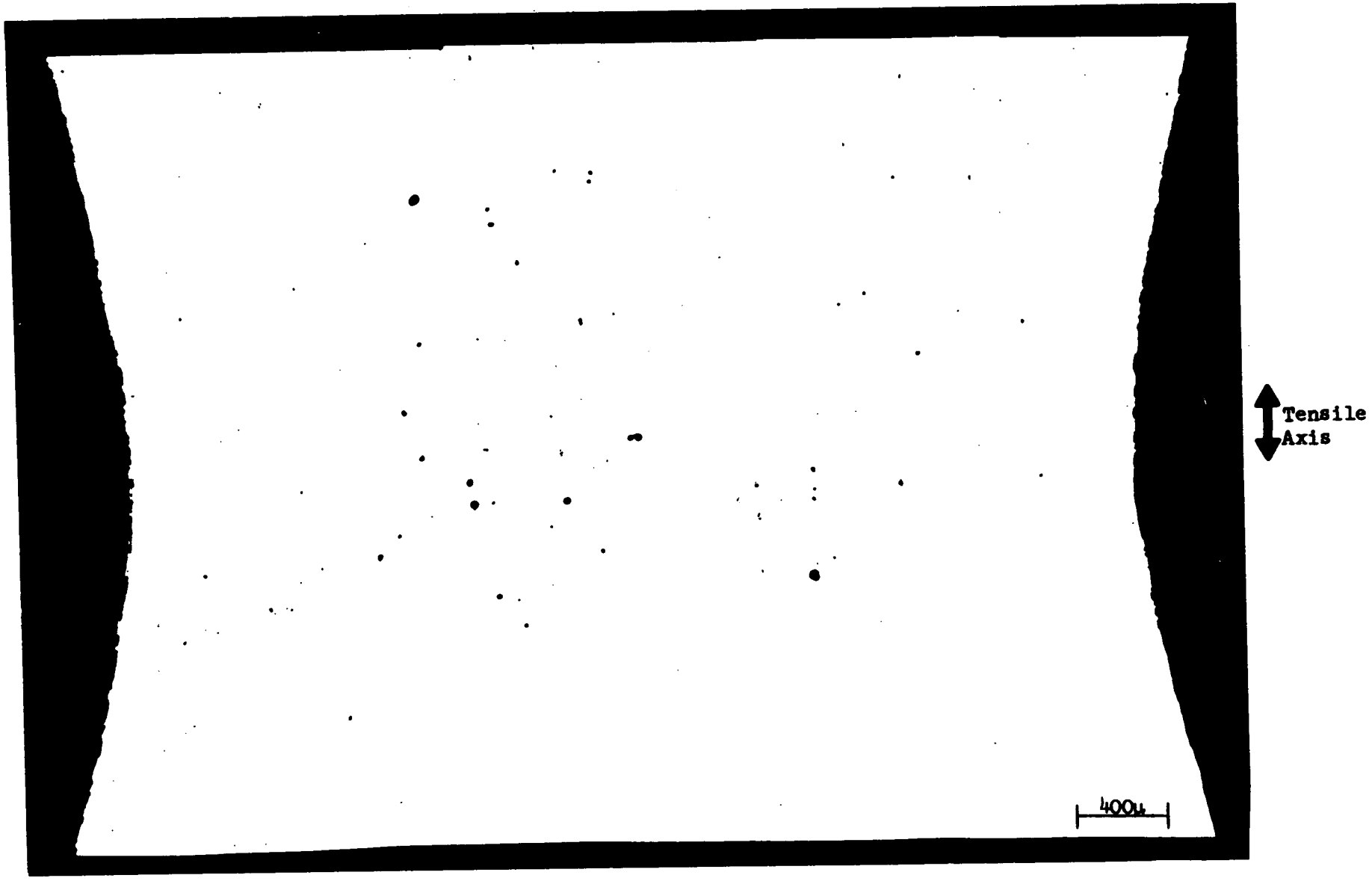

Figure 18 Midplane of Neck of Commercial 18 Ni Maraging Plastically Strained 58 Percent

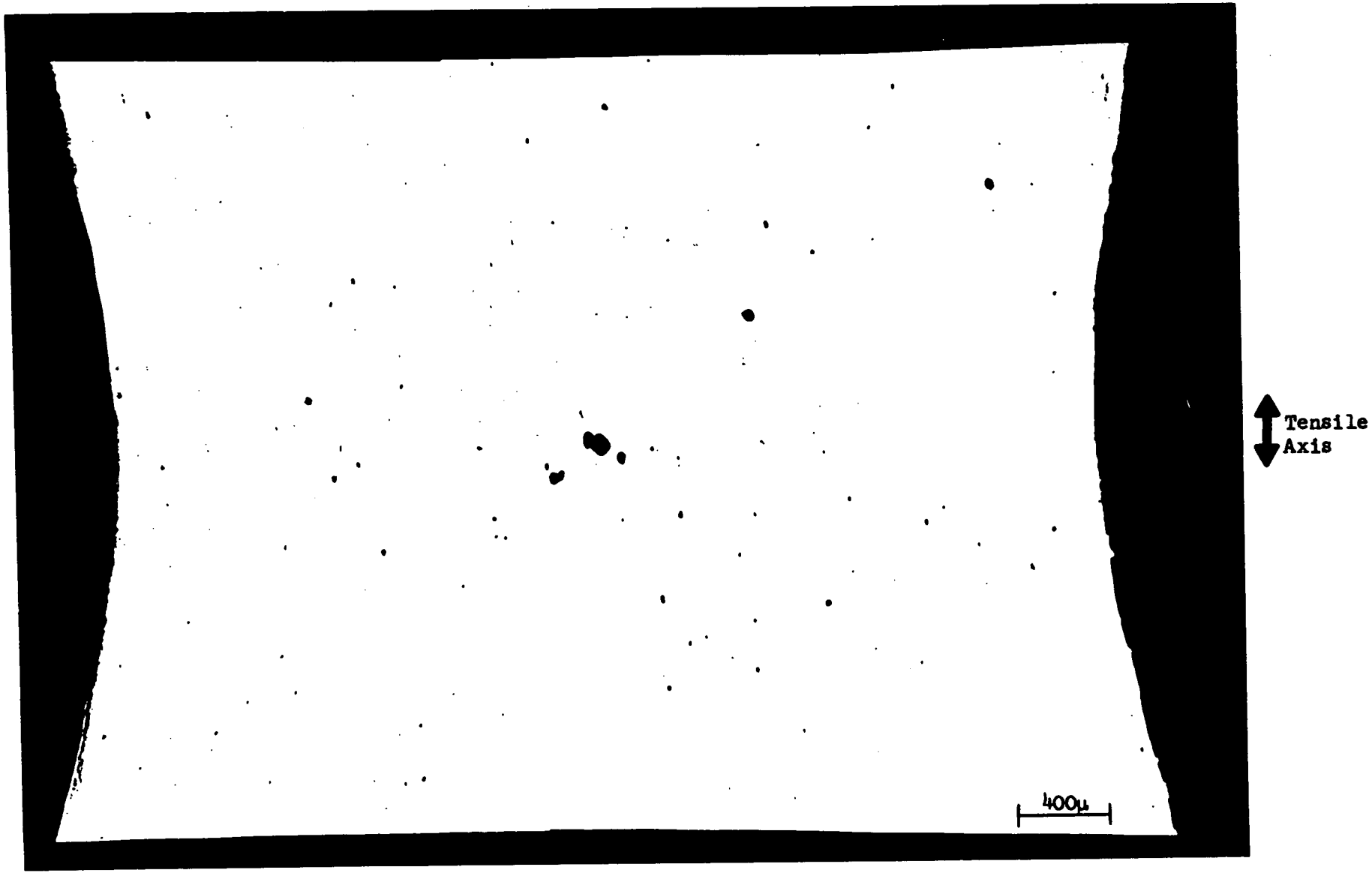

Figure 19 Midplane of Neck of Commercial 18 Ni Maraging Plastically Strained 62 Percent

central portion of the neck of the maraging specimens grow almost symmetrically at higher strains, while those near the edge or those lying outside the neck tend to be elongated in the direction of the applied tensile stress. Voids near the edge or away from the neck exhibit no appreciable sideways growth even at very high strains, while those in the center grow longitudinally at low strains but begin to exhibit lateral growth at high levels of plastic strain. Figures 20 and 21 illustrate these observations for the commercial grade maraging steel.

Thus, qualitatively, the void growth process appears to be very similar in all four alloys. At low strains, the void nuclei tend to grow in the direction of the applied tensile stress. As straining continues, a substantial neck is formed resulting in a triaxial state of stress in the center of the tensile specimen. In the presence of the triaxial state of stress, the voids in these alloys tend to grow more uniformly, exhibiting lateral or radial growth as well as the earlier established longitudinal growth. Those voids which lie outside the regions of substantial triaxiality (those towards the specimen edge or lying outside the necked region) continue to grow preferentially in the direction of the applied tensile load.

No effort has been made to correlate the exact stress states at particular points along the minimum diameter (known from the Bridgman analysis[4]) with the sizes of voids present. It is demonstrated below that the void initiation and growth processes are very much dependent on inclusion size. Thus, the size of void present at a particular location is a function not only of the stress state at the point but also is

a. Plastically Strained
18 Percent

b. Plastically Strained
58 Percent

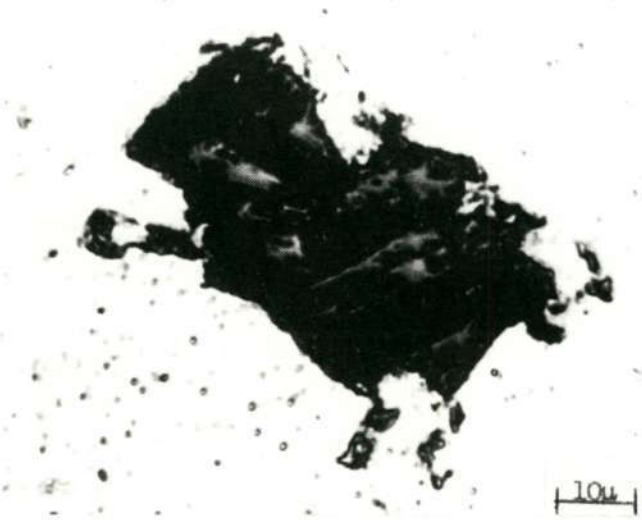

c. Plastically Strained
66 Percent

Figure 20 Voids in the Centers of Tensile Specimens of Commercial 18 Ni Maraging Plastically Strained

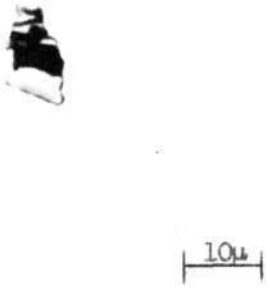

a. Plastically Strained
18 Percent

b. Plastically Strained
58 Percent

c. Plastically Strained
66 Percent

Figure 21 Voids on the Edge of Tensile Specimens of Commercial 18 Ni Maraging Plastically Strained

dependent on the size of inclusion that happens to lie at that particular point. The spacial distribution of inclusion sizes is assumed to be random in these alloys. Hence, considering the probability of the existence of inclusions of one particular size, shape, and orientation at specific locations, it is not possible to correlate void sizes quantitatively with the exact stress states in this study.

VOID COALESCENCE

It has been seen that qualitatively the processes of void initiation and growth in these two alloy families are not essentially different. Yet, as shown previously,[3] the fracture toughness values vary quite widely in these alloys with the maraging steels being substantially tougher than the AISI 4340 alloys. A possible explanation for this difference lies in the fundamental differences observed in the void coalescence processes of these two alloy systems.

Just as has been reported above that the void initiation and growth stages occur simultaneously as straining proceeds, so also concurrently with the initiation and growth of voids, these voids begin to coalesce at high levels of strain, preferentially in the center of the specimen. The process of coalescence in the AISI 4340 alloys involves the linking of adjacent large voids by narrow cracks. The first appearance of the cracks is observed in both the commercial and high purity alloys at approximately 90 percent of the fracture strain. A photomicrograph of the early stages of void coalescence in the commercial AISI 4340 alloy is presented as Figure 22. Many of the cracks joining adjacent voids in the quenched and tempered steels were oriented at approximately 45° to the tensile axis in this section, as is illustrated in Figure 23, although their orientation in three dimensional space is unknown. At strains within one or two percent of fracture, the coalescence of voids in the central region of the tensile specimen neck is extensive enough to form a rather large continuous cavity spanning as

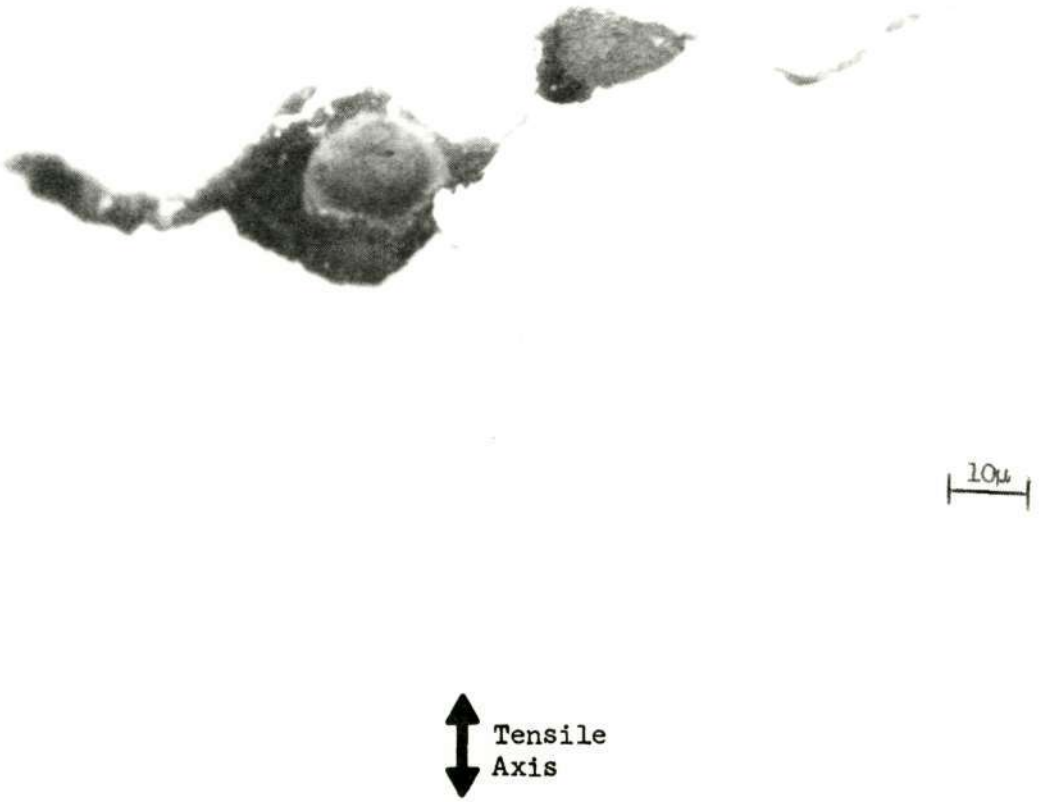

Figure 22 Coalescence of Voids by Cracking in Commercial AISI 4340 Plastically Strained 25 Percent

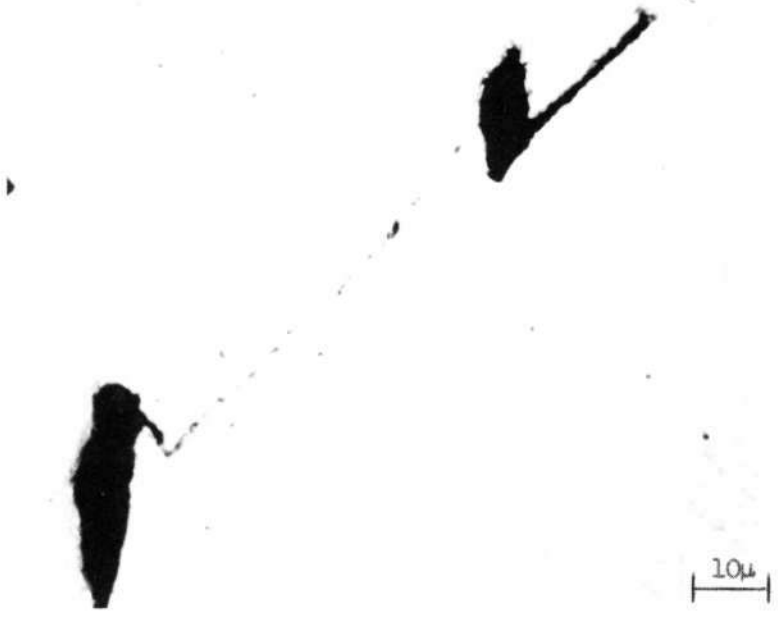

a. Plastically Strained 25 Percent

b. Plastically Strained 27 Percent

Figure 23 Coalesence of Voids by 45° Cracks in Commercial AISI 4340 Plastically Strained

much as five percent of the specimen diameter. An example of such a cavity is presented in the composite photomicrograph of Figure 24.

While the path followed by the narrow cracks in the AISI 4340 cannot be determined from the above photomicrographs, the fractographic study previously reported[3] provides the answer. The fracture surfaces of the AISI 4340 alloys were covered with large dimples nucleated by the sulfide inclusions separated by extensive areas of very fine dimples nucleated by the strengthening carbides in the quenched and tempered structure. Apparently, these narrow cracks which link up large voids, formed at the sulfides, follow the path of a series of small voids nucleated at the carbide particles. As may be seen in Figure 6, the small voids coalesce by growing until they impinge on each other and thus create the cracks. The previous report also demonstrated the tendency of the fracture to follow the ferrite-ferrite boundaries where the carbide density is thought to be highest. Thus, in the AISI 4340 alloys, growth of the voids nucleated at sulfide inclusions in the central region of the specimen continues until rather narrow cracks formed by linkup of voids initiated at the carbides results in the coalescence of the large voids. This cracking process is perhaps similar to that described by Rogers[5] as "void sheet" formation in copper. Puttick[6] also observed narrow cracks linking large voids in strained specimens of iron containing 0.026 weight percent carbon. Once coalescence has begun, a central cavity is quickly formed in the tensile specimen and final fracture results shortly thereafter. As yet, the critical conditions for crack formation have not been determined, but they must undoubtedly

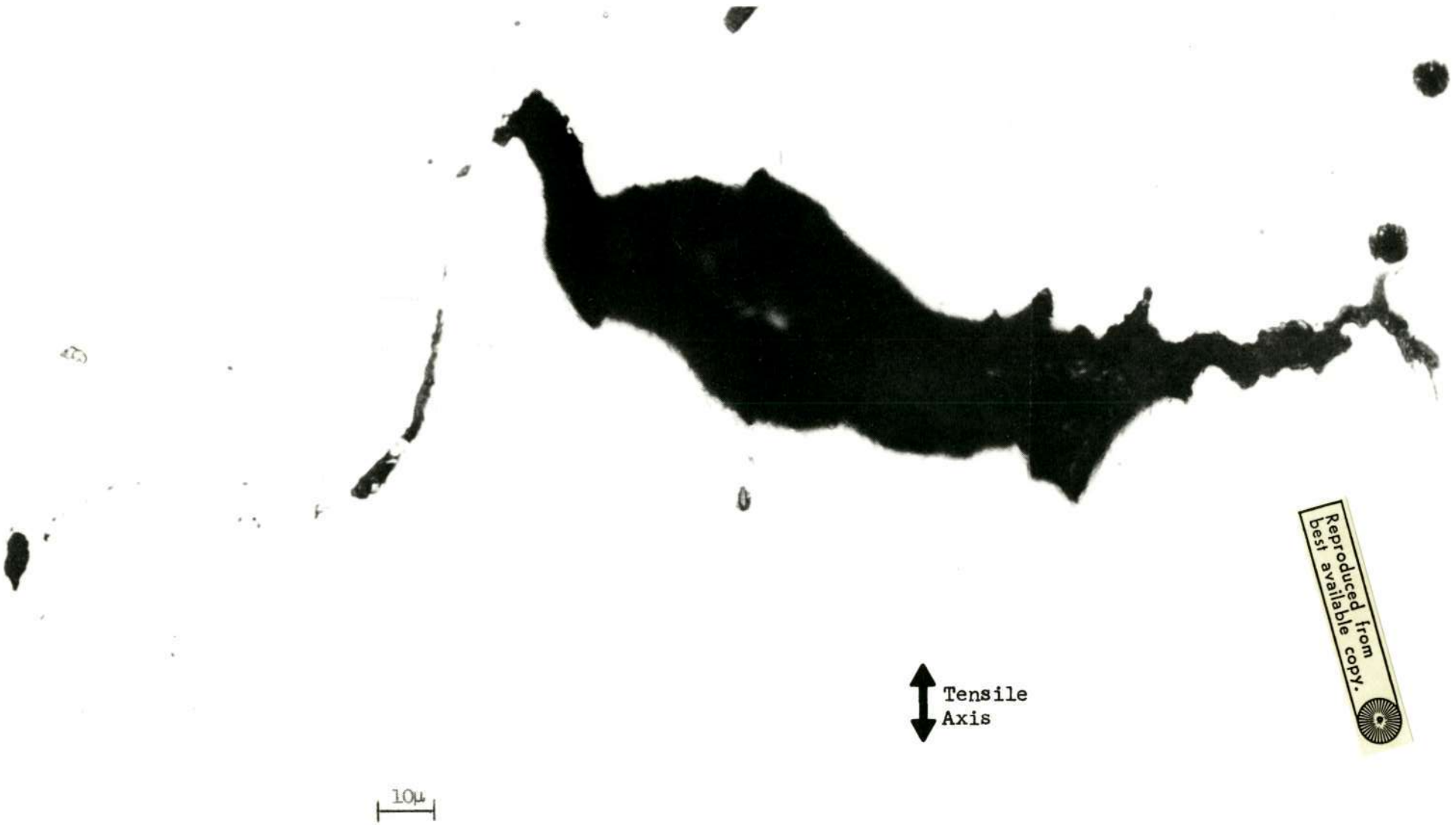

Figure 24 Central Cavity in Commercial AISI 4340 Plastically Strained 27 Percent

involve the concentration of a critical shear stress in the region between two adjacent, growing, large voids.

In contrast to the mechanism of coalescence described above, voids in the central portion of the maraging specimens seem to grow continuously with increasing strain until they impinge on each other. This behavior of literally growing into one another had been suggested as a possible mechanism of void coalescence by Cottrell.[7] The first appearance of coalescence of the voids in both the maraging steels occurs at strains of approximately 80 percent of the fracture strain. An example of voids coalescing in the high purity maraging steel is presented in Figure 25. As straining continues, the void coalescence process leads to the formation of a large central cavity, as illustrated for the commercial maraging steel in Figure 26. Once a cavity as long as 5 to 10 percent of the minimum specimen diameter is formed, final fracture occurs rapidly.

Thus, there has been observed a fundamental difference in the mechanisms by which inclusion-nucleated voids coalesce in these two families of steels. Coalescence occurs in the AISI 4340 alloys by the formation of cracks connecting carbide particles which lie between the sulfide inclusions. The process by which the voids in the maraging steels coalesce is simply the continued growth of the voids until they impinge on each other. Once a central cavity has formed in any of the alloys, final fracture occurs rapidly within only one or two more percent plastic strain.

Figure 25 Void Coalescence in High Purity 18 Ni Maraging Plastically Strained 81 Percent

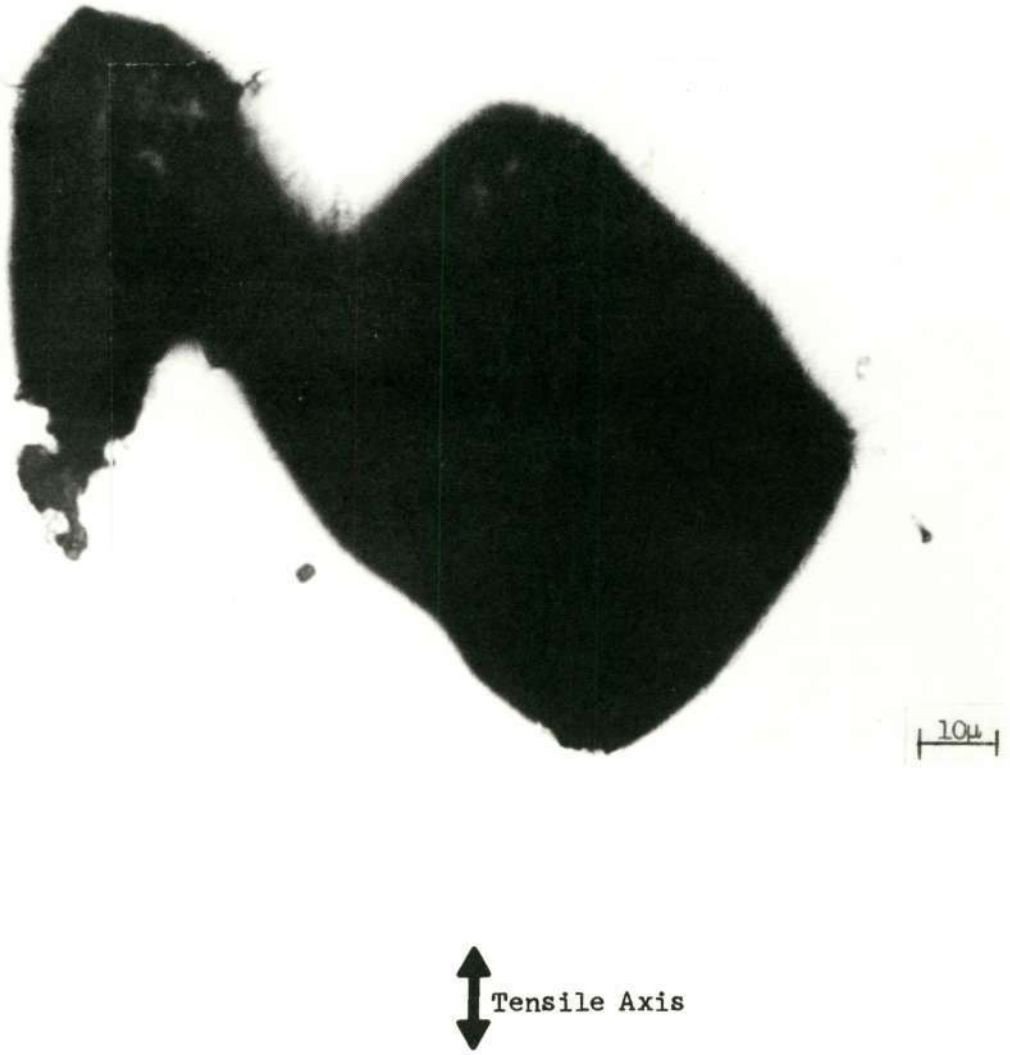

Figure 26 Central Cavity in Commercial 18 Ni Maraging Plastically Strained 61 Percent

QUANTITATIVE METALLOGRAPHY

A quantitative metallographic investigation was carried out using the strained and sectioned tensile specimens to quantitatively describe the void initiation and growth processes. Since the stress state varies with position on the midplane of the tensile neck, it was decided to arrive at some sort of average measurements by completely examining predetermined areas in the centers of the midplanes. To determine the areas from which measurements would be made, fractured tensile halves of each alloy, sectioned to expose the midplanes, were examined. As is seen in the photomicrographs of the nickel plated fractured tensile specimens presented in Figures 27-30, the presence of large voids is not limited to the fracture path, but rather voids extend away from the fracture surfaces in the direction of the tensile axis. To provide measurements which offer an average of stress conditions found in the neck yet are pertinent to the fracture process, an area centered on the point of intersection of the minimum diameter of the neck and a longitudinal bisector of the specimen was metallographically examined. The dimensions of the area varied from alloy to alloy. These dimensions were chosen with reference to the fractured tensile halves so that the longitudinal dimension of the area extended to include all voids of substantial size away from the fracture surface, and the transverse dimension of the area was taken as the width of the area of normal rupture on the fracture surface, i.e., the shear lips are not included.

As may bee seen in the photomicrographs of the tensile halves, the extent of the presence of large voids is greater for the commercial

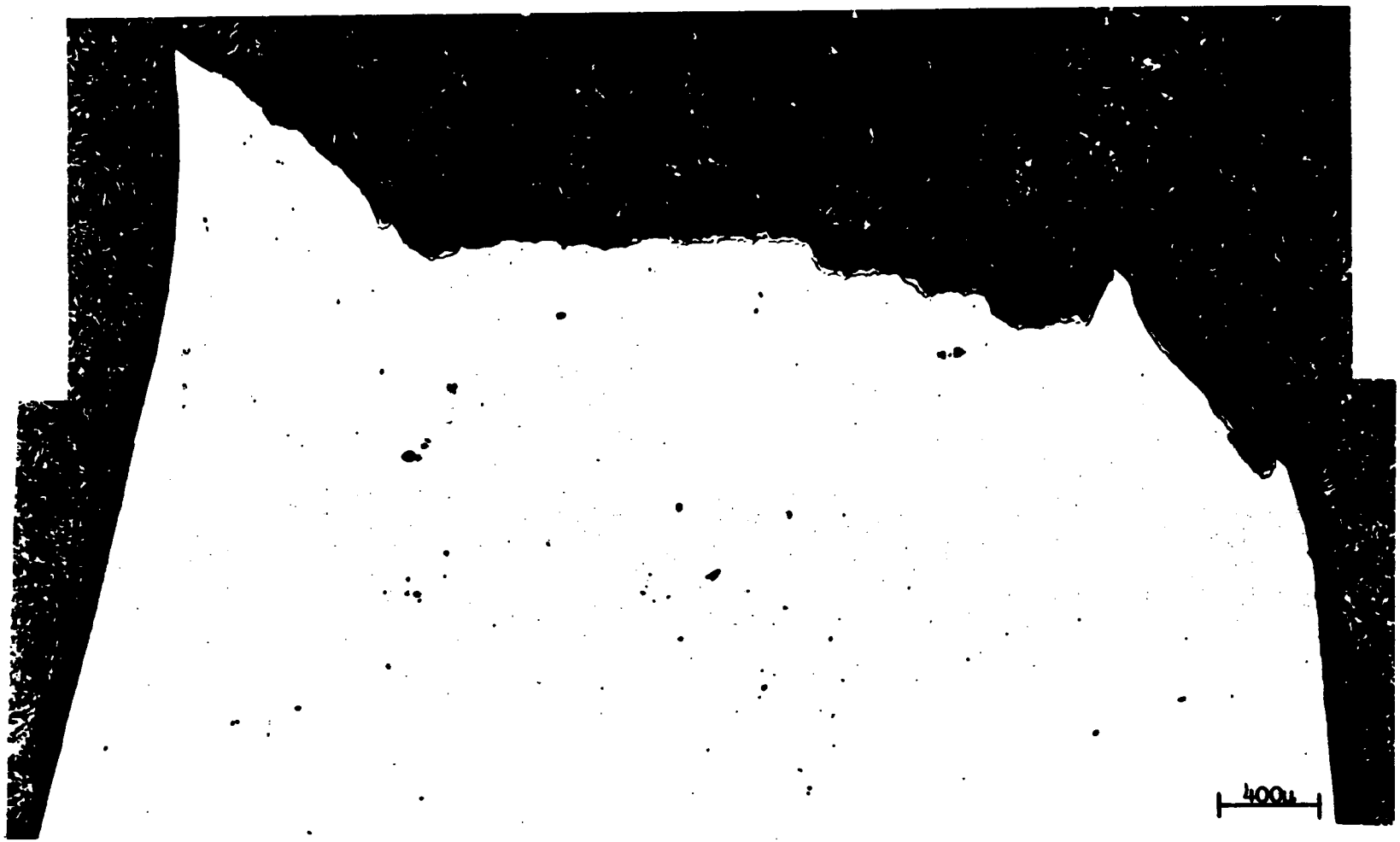

Figure 27 Midplane of Fractured Tensile Specimen of Commercial AISI 4340 (ϵ = 0.288)

Figure 28 Midplane of Fractured Tensile Specimen of High Purity AISI 4340 (ϵ = 0.498)

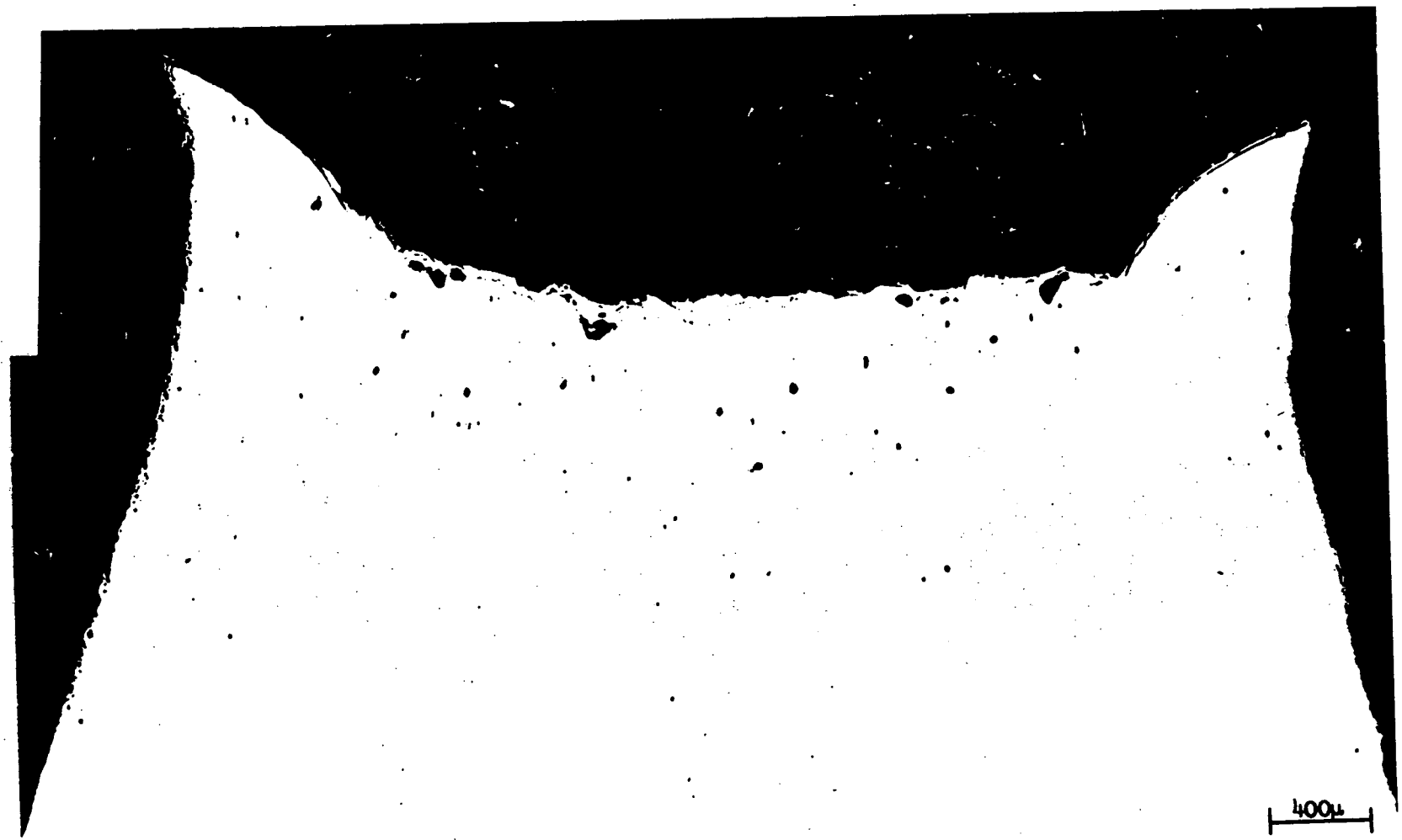

Figure 29 Midplane of Fractured Tensile Specimen of Commercial 18 Ni Maraging (ϵ = 0.728)

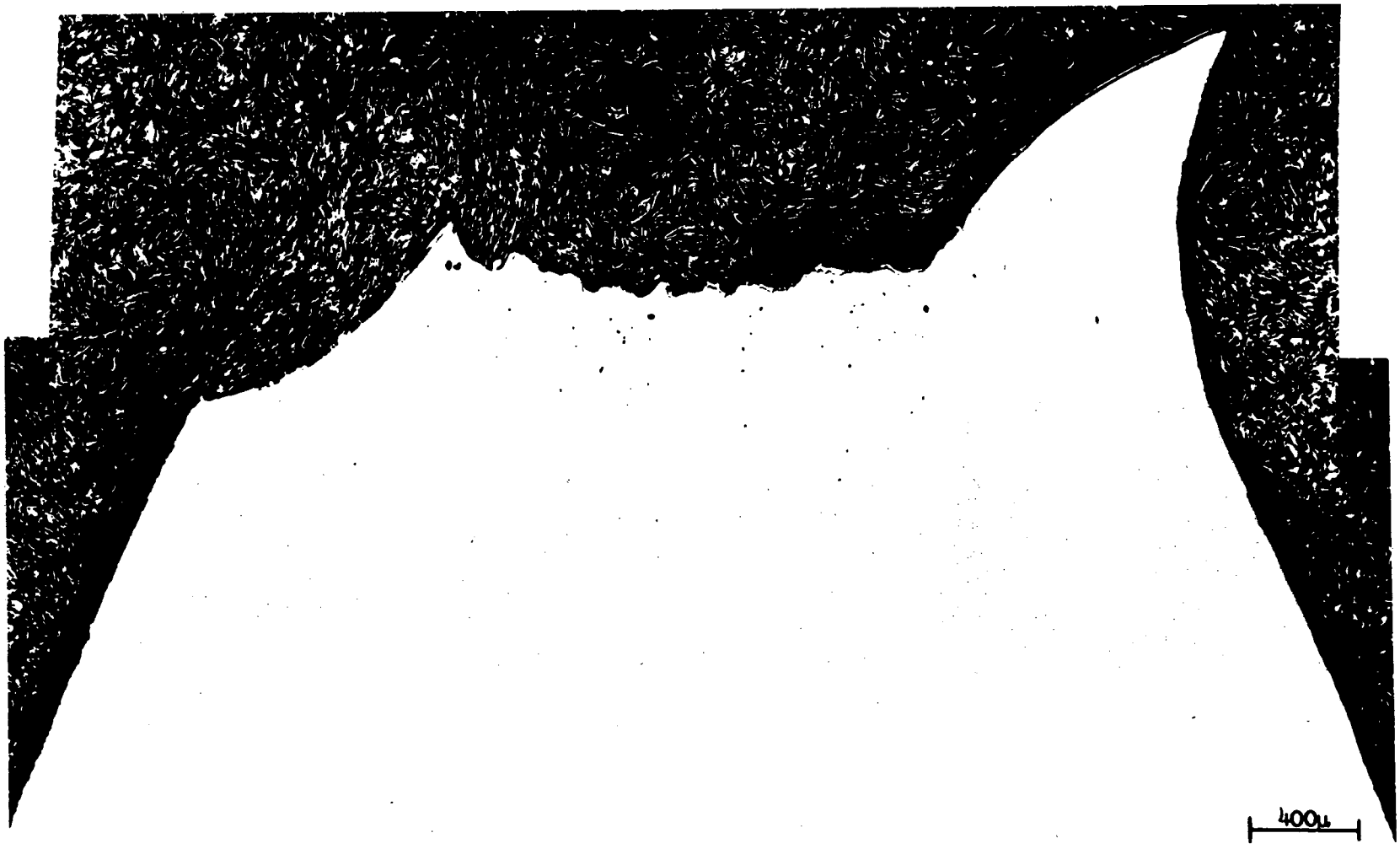

Figure 30 Midplane of Fractured Tensile Specimen of High Purity 18 Ni Maraging (ϵ = 0.970)

alloys than for the high purity alloys. This fact is shown quantitatively in Table II where the exact sizes of the areas examined in each alloy are tabulated. It is also seen in Table II that the size of the area of major void formation decreases continuously from the least tough alloy, commercial AISI 4340, to the most tough, high purity 18 Ni maraging.

The procedure followed in the quantitative metallographic investigation involved viewing each square micron of the predetermined area of the midplane in a strained and sectioned tensile specimen. The image of an area 0.15 mm x 0.20 mm was projected on a ground glass screen on the metallograph at a magnification of 1000X. Using graduated controls on the specimen stage for specimen translation, this projected microscopic area was made to translate over the entire macroscopic areas listed in Table II. In each microscopic area, the number of inclusions present were counted together with the number of voids present and the number of inclusions with associated voids. Once these measurements had been made, a transparent sheet with a square point grid of 0.5 cm spacing was placed over the screen and the number of intersections of the grid and the voids present was determined. Using standard quantitative metallographic calculations,[8] it was then possible to determine the area fraction of the test section covered by voids. The above measurements permit calculation of the percent of inclusions which have voids associated with them at each level of strain for each of the alloys. This quantity is a measure of the extent of void nucleation. Using the calculated area fractions of voids intersected by the test plane together

TABLE II

Dimensions of Areas Metallographically Examined in Strained Tensile Specimens

Alloy	Length(mm)	Width(mm)
Commercial AISI 4340	2.25	3.00
High Purity AISI 4340	2.10	2.80
Commercial 18 Ni	2.15	2.60
High Purity 18 Ni	1.95	2.00

with the total number of voids present, it was possible to calculate the average cross-sectional area of void intersected by the midplane. This quantity is, in fact, a measure of the average size of void present and thus is a measure of the extent of void growth. This particular measure was chosen since the voids are generally irregular in shape such that some average linear dimension of the voids, e.g., diameter, has questionable meaning. By recording the data for each microscopic area examined, it was possible to determine the effects of location in the neck on void initiation and growth.

The results for the percent of inclusions which had voids associated with them are presented in Figure 31. Each datum point represents observations from at least 110 inclusions. The plots indicate that for all alloys, except the commercial purity 18 Ni, void initiation is a continuous process up to fracture (values taken from fractured specimens are indicated by "F"). In the commercial 18 Ni maraging steel, all of the inclusions in the critical zone had nucleated voids at strains approximately 15 percent below the fracture strain. The commercial purity alloys (open symbols) show initiation of voids at lower strains than do the high purity alloys (solid symbols). It should also be noted that the commercial grade 18 Ni, 200 grade maraging steel (open triangles) had 19.3 percent of its carbo-nitride inclusions fractured before any load was applied, i.e., in the as-received condition. The slopes of the plots indicate that the rate of void initiation is greater for the commercial alloys than for the high purity, which is probably due to the larger sizes of inclusions found in the commercial steels. The order of the slopes for

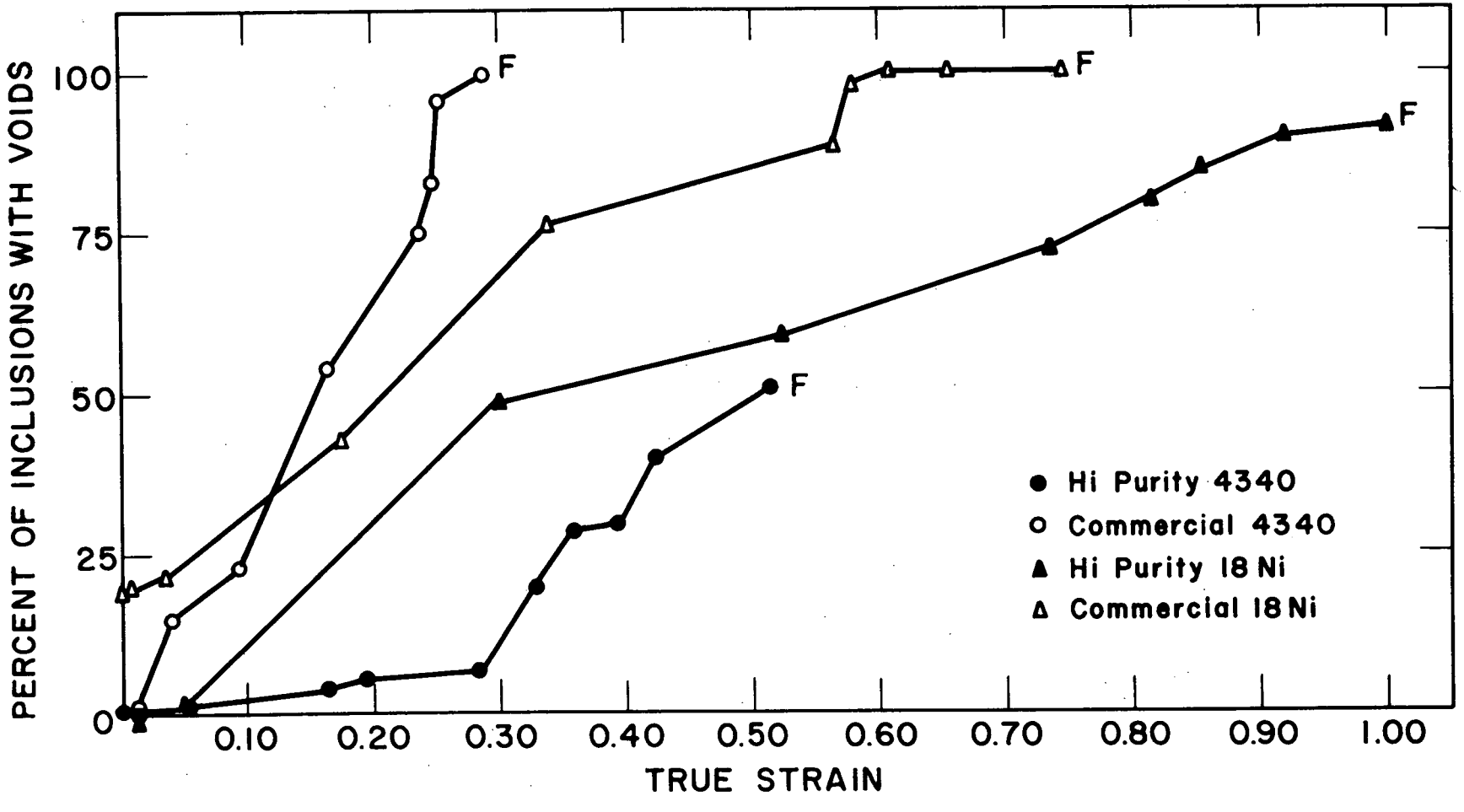

Figure 31 Extent of Void Initiation—Percent of Inclusions with Voids as a Function of True Strain (F indicates value taken from fractured specimen)

all four alloys follows the order of the fracture toughness values with the exception of the high purity AISI 4340 (solid circles). The least tough alloy, commercial grade AISI 4340 (open circles), exhibits the highest rate of void initiation. The apparent misplacement of the plot for high purity AISI 4340 is probably due to the very wide distribution of inclusion sizes found in this alloy. It was observed for the high purity alloys that even at the fracture strains, not all of the inclusions present in the critical area had nucleated voids. Generally, the small inclusions of approximately one micron in linear dimension showed no void initiating ability. Careful tabulation of the location of void nucleating inclusions indicated that there is no apparent dependence of void initiation on position in the tensile neck. The continuous process of void initiation is the result of smaller and smaller inclusions becoming active as void nucleating sites as the strain is increased.

Figure 32 presents the average cross-sectional area of void intersected by the midplane as a function of strain. The average cross-sectional area per void is a measure of the average size of void present and as such gives a measure of void growth with strain. Each of the plots of Figure 32 shows a long linear initial portion where the average size of void increases continuously with strain. At strains within about 5-10 percent of fracture, the plots generally show a rapid increase in the size of voids present. This rapid jump corresponds with the onset of void coalescence and the formation of the central cavity in the tensile specimen. The slopes of the plots indicate that the rates of void growth follow the order that would be expected from the toughness

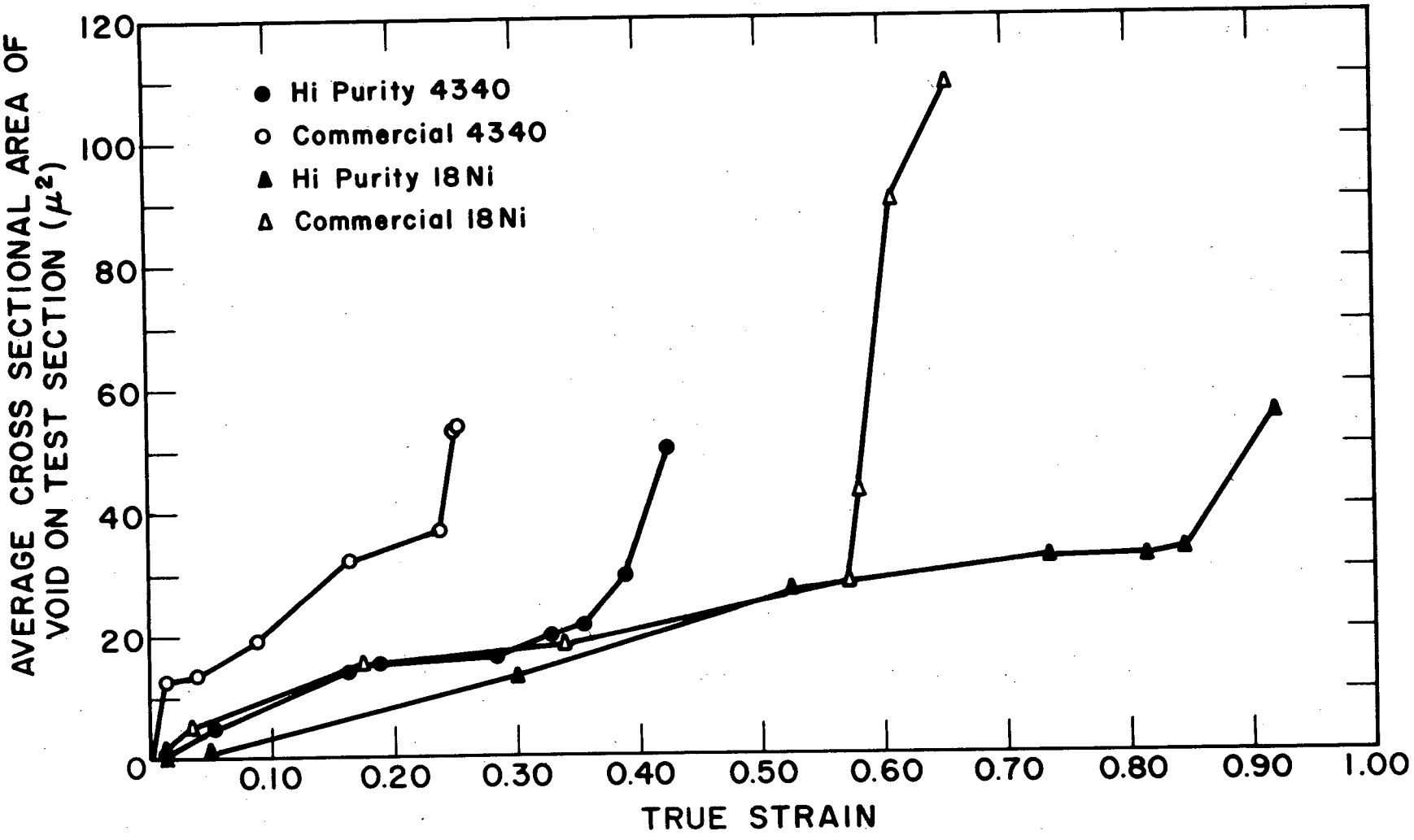

Figure 32 Extent of Void Growth—Average Cross Sectional Area of Void as a Function of Strain

levels of the four alloys. The commercial grade AISI 4340 (open circles), which is the least tough alloy, exhibits the highest rate of void growth, while the high purity maraging steel (solid triangles), which is the most tough alloy of the four, exhibits the lowest rate of void growth. The order of void growth rates also corresponds to the order of the sizes of inclusions present in the alloys, indicating that void growth proceeds more rapidly from the larger inclusions. Location within the neck definitely affects void growth. The voids near the centers of the necks grew at higher rates and to much greater sizes than the average values. These observations indicate that for the magnitude of the variation in hydrostatic tension attainable from edge to center of smooth, round tensile specimens, there is no affect of hydrostatic stress on void initiation. On the other hand, the hydrostatic stress enhances void growth.

DISCUSSION

The above results indicate that the size of the non-metallic inclusions is a very important factor in the fracture behavior of these alloys. Void initiation occurs first at the large particles, and void growth proceeds more rapidly from the large particles. The result is that the high purity alloys, which have much smaller non-metallic inclusions than the commercial alloys, are more resistant to plastic fracture. This fact suggests the possibility of designing new processing techniques for reducing the sizes of inclusions in these alloys in order to improve their fracture toughness values.

Palmer, Smith, and Warda[9] observed void initiation to occur first at the largest oxide particles in internally oxidized copper alloys. They reasoned that stress concentrations set up by the blocking of dislocations at the inclusions would be greatest at the large particles, since dislocations would be less able to cross slip around the large inclusions. This explanation for the observation that the large inclusions nucleate voids first is probably not as applicable to the alloys being considered in this study as it was for the copper alloys used by Palmer, et. al. The inclusions in these high strength steels vary in size from approximately 1 to 15 microns, substantially larger than the particles in the copper alloys, and also very large distances for dislocations to cross slip considering the fine nature of the martensitic structures and very high dislocation densities found in these alloys. Likewise, arguments involving the interparticle spacing and the length of dislocation pile-ups would not be applicable, since

the average distances between inclusions is of the order of tens of microns, substantially greater than the martensitic platelet sizes found in these alloys.

It has been demonstrated in the past that for brittle materials the fracture stress decreases as the size of the material increases.[10] This behavior is related to the greater probability of finding critical flaws in a large volume of material. This sort of an argument may have some merit regarding these steels. The titanium carbo-nitrides in the maraging alloys are brittle and have been shown to nucleate voids by cleavage failure of the inclusions (note example in Figure 10). Thus, the larger inclusions may nucleate voids first in the maraging steels because they fracture at lower stresses due to the presence of critical flaws in the inclusions. If the interface between the steel matrix and the sulfide inclusions, which fails in order to produce voids in the AISI 4340 alloys, may also be considered a brittle material, this same explanation seems to be consistent for the quenched and tempered steels also. As the size of the sulfide increases, the total volume of sulfide-matrix interface also increases; thus the probability of finding a defect or weak area in the boundary is greater.

The heat treatments given these alloys involve rapid rates of quenching from the austenitizing temperatures in order to insure transformation of the structures to martensite. The differences in coefficients of thermal expansion between the matrix materials and the inclusions undoubtedly lead to stress concentrations within the inclusions and at the matrix-inclusion interfaces as a result of heat treatment. Coupled with

this effect are the stresses on the inclusions which are obviously introduced by the rapid expansion of the matrix during the martensitic transformation. These imposed stress concentrations, while macroscopically compressive, could conceivably result in localized tensile stress concentrations or the introduction of cracks in the inclusions or at the interfaces. Some evidence for this process is provided by the fact that approximately 20 percent of the inclusions (generally the largest present) in the commercial maraging steel were cracked before tensile straining. While one would expect the larger brittle inclusions to be more susceptible to damage from thermal shock, it is not so obvious, because of the complexity of the problem, that the stresses set up within the inclusions and at the interfaces due to the thermal treatments and matrix transformations would necessarily be greater for the larger sized inclusions. Further work in this particular area may provide for a better understanding of the reasons for the effect of inclusion size on void nucleation.

The observation of the rate of void growth being greater at the larger particles may simply be the result of increased stress due to a reduced cross-sectional area. Once an inclusion has failed or the interface has failed between an inclusion and the matrix, the newly created free surface area is no longer available to help carry the applied load. Thus, not only is the stress concentrated by a void due to the discontinuity in the material (which is constant for any given geometry of void regardless of size), but the stress is further increased in the alloy which has more and larger newly initiated voids due to a

greater reduction in the sound cross-sectional area available to carry the load. Once a void begins to grow, this process continues to increase the stress on the matrix resulting in further plastic flow and void growth. Thus, those voids which are born larger should grow faster and this is what has been observed. The continuum mechanics approach to void growth as treated by McClintock[11] and Rice and Tracey[12] also predicts a direct dependence of the rate of void growth (defined here as $dR/d\epsilon$) on the initial void size.

One other observation should be discussed concerning the results of this study. It is a generally observed fact that the maraging steels as a family are tougher at a given strength level than the quenched and tempered steels. The current study seems to indicate that this difference may be due to the fact that the growth of voids nucleated by the non-metallic inclusions in the AISI 4340 alloys is interrupted before impingement by the formation of cracks which connect the voids. These cracks have been shown to follow a path of fine voids nucleated by the strengthening carbides. In contrast, the strengthening particles in the maraging steels do not initiate a population of voids so that inclusion-nucleated voids grow until impingement. Thus, fracture in the maraging steels occurs at higher strains than in the AISI 4340 alloys. The particles of intermetallic compound which strengthen the maraging steels are one to two orders of magnitude smaller than the carbides in the quenched and tempered steels. The concept that the smaller particles may permit some stress relaxation at the matrix-particle interface by the cross slip of dislocations is probably valid for these strengthening

precipitates. The interface between the intermetallic and the maraging matrix may also be stronger than the carbide-matrix interface in the quenched and tempered steels. In any event, these observations suggest that it may be possible to alter the carbide dispersion in the quenched and tempered steels in order to prevent or delay nucleation of voids at the carbide interface. As a first attempt, it would be advantageous to reduce the size of the carbides and perhaps produce a more homogeneous dispersion since the carbides tend to precipitate at the ferrite-ferrite boundaries.[13] There is evidence that this approach may work in the fact that both strength and toughness can be improved in certain steels by various thermomechanical treatments which result in redistribution of the carbides off the lath boundaries and refinement in the size of the carbides.[21] Whether or not this is possible in AISI 4340 remains to be demonstrated.

CONCLUSIONS

The following conclusions may be drawn from the work completed during this report period:

1) The macroscopic flow characteristics of the four alloys, as described by the shapes of their tensile flow curves, are quite similar.

2) Void initiation at sulfide inclusions in the AISI 4340 alloys occurs predominantly by decohesion along the matrix-sulfide interface.

3) Void initiation at small carbide precipitates in the AISI 4340 alloys takes place by decohesion along the matrix-carbide interface.

4) Void initiation at carbo-nitride inclusions in the 18 Ni maraging steels takes place exclusively by fracturing of the inclusions.

5) Void initiation in all four alloys is unaffected by the level of hydrostatic tension attainable in a smooth, round tensile specimen.

6) Void growth in all four alloys is enhanced by increased hydrostatic tension as indicated by the larger sizes of voids found in the center of round necked tensile specimens.

7) Void coalescence in the AISI 4340 alloys occurs by the linking up of inclusion-nucleated voids by cracks which follow paths of fine voids nucleated by the carbide precipitates.

8) Void coalescence in the 18 Ni 200 grade maraging steels occurs by a mechanism of void growth until impingement.

9) Larger inclusions in these four alloys result in earlier void initiation and more rapid void growth.

FUTURE WORK

Although the classic experiments of Bridgman[14] and the later work of Marshall and Shaw[15] and Coffin and Rogers [16] have demonstrated that increased ductility can be achieved by reducing the level of hydrostatic tension, the exact mechanism by which hydrostatic tension affects the fracture process has not been determined. The qualitative results reported above tend to indicate that increased hydrostatic tension aids void growth while not affecting the nucleation of voids. However, the variation in the hydrostatic component of stress from the center of a 1/4 inch, smooth, round tensile specimen to the edge is not sufficient to conclusively demonstrate the effects of hydrostatic tension. With the purpose of quantitatively and systematically defining the effects of hydrostatic tension on the fracture process, it is proposed that a metallographic study similar to the one reported herein be carried out on the four alloys using notched round tensile specimens. The work of several investigators indicates that it will be possible to increase the level of hydrostatic tension substantially above that for smooth rounds using mildly notched specimens.[17, 18, 19] The specimen geometry will be chosen so as to give the maximum increase in hydrostatic tension while maintaining a stress state as similar to that in the smooth specimens as possible. Also, the geometry will be chosen to guarantee fracture initiation in the center of the specimen. Comparison of the results with those from the smooth round investigation should conclusively demonstrate the mechanism by which hydrostatic tension affects fracture in these alloys.

Since the difference in void coalescence mechanisms between the maraging alloys and the AISI 4340 alloys seems to be the primary reason for the difference in toughness levels, it is proposed to study the coalescence stage further. In particular, an attempt will be made to better understand the cracking mechanism in the AISI 4340 alloys. The study will involve examination of tensile sections using surface replicas and both electron microscopy and high magnification light microscopy to see if the strain patterns between large voids offers help in understanding the cracking process. Transmission electron microscopy may also be used further to study the nucleation and growth of voids at the carbide particles in the AISI 4340 alloys.

REFERENCES

1. J. Plateau, G. Henry and C. Crussard, Revue Me'tall., 54 (1957) p. 200.

2. J. R. Low, Jr., Engr. Frac. Mech., 1 (1968) p. 47.

3. T. B. Cox and J. R. Low, Jr., "Investigation of the Plastic Fracture of High Strength Steels", NASA Technical Report No. 3 on Research Grant NGR 39-087-003 (May 1972).

4. P. W. Bridgman, Large Plastic Flow and Fracture, McGraw-Hill, New York (1952) p. 9.

5. H. C. Rogers, Trans. AIME, 218 (1960) p. 498.

6. K. E. Puttick, Phil. Mag., 4 (1959) p. 964.

7. A. H. Cottrell, in Fracture, eds. Averback, Feldbeck, Hahn, and Thomas, John Wiley, New York (1959) p. 20.

8. E. E. Underwood, Quantitative Stereology, Addison-Wesley, Reading, Mass. (1970) p. 24.

9. I. G. Palmer, G. C. Smith, and R. D. Warda, Inst. Phys. Conf. Ser. 1, Oxford (1966) p. 53.

10. N. Davidenkov, E. Shevandin, and F. Wittmann, Trans. ASME, 69 (1947) p. A63.

11. F. A. McClintock, Jnl. Appl. Mech., 35 (1968) p. 363.

12. J. R. Rice and D. M. Tracey, Jnl. Mech. Phys. Solids, 17 (1969) p. 201.

13. A. J. Baker, F. J. Lauta, and R. P. Wei, Structure and Properties of Ultrahigh-Strength Steels, ASTM STP 370 (1965) p. 3.

14. P. W. Bridgman, Ibid, p. 38.

15. E. R. Marshall and M. C. Shaw, Trans. ASM, 44 (1952) p. 705.

16. L. F. Coffin and H. C. Rogers, Trans. ASM, 60 (1967) p. 672.

17. A. W. Dana, E. L. Aul, and G. Sachs, NACA Tech. Note 1830 (1949).

18. J. D. Lubahn, from Fracturing of Metals, ASM (1948) p. 90.

19. D. P. Clausing, Jnl. Mat., 4 (1969) p. 566.

REFERENCES (continued)

20. A Considère, Ann. ponts et Chaussées, 9 (1885) p. 574.

21. M. J. May and D. J. Latham, "Thermomechanical Treatment of Steels" in Toward Improved Ductility and Toughness, Climax Molybdenum Development Company (Japan) (1971) p. 157.